EFFECTS OF NEUROINFLAMMATION ON VASCULAR DYSFUNCTION IN ALZHEIMER'S DISEASE

A Dissertation
Presented to
The Academic Faculty

by

Johnathon Robert Long

In Partial Fulfillment
of the Requirements for the Degree
Masters of Science in the
BioEngineering

Georgia Institute of Technology
May 2017

EFFECTS OF NEURONINFLAMMATION ON VASCULAR DYSFUNCTION IN ALZHEIMER'S DISEASE

Approved by:

Dr. Levi B. Wood, Advisor
School of Mechanical Engineering]
Georgia Institute of Technology

Dr. Young Jang
School of Biological Sciences
Georgia Institute of Technology

Dr. Tony Kim
School of Mechanical Engineering
Georgia Institute of Technology

Date Approved: April 27, 2017

ACKNOWLEDGEMENTS

I would like to start by mentioning that I am thankful for all the advice and support from my advisor, thesis committee, friends and family. I do not think that I would have such an enriched education and life without all the people that have provided me with an environment to nurture my educational growth and development.

I would like to thank Dr. Levi Wood for everything he has taught me about the many aspects of computational bioengineering. Working in his lab has provided me with a breadth of exposure to biological applications that will prove to be advantageous in my future career. I would also like to attribute to Dr. Wood the unlocking of my mind to the limitless potential for scientific discovery, leading to my development as a committed, driven and devoted scientist and engineer. I would like to thank Dr. Young Jang for providing expert advice on the development of my own research project and willingness to collaborate to help propel the progress of my project. Also, Dr. Jang's willingness to share lab equipment has enabled me to analyze additional metrics of endothelial cells. I would also like to thank Dr. Tony Kim to being highly receptive and supportive of my project's design. He was one of the first professors that I met at Georgia Tech and helped convince me that I had made the correct decision to attend Georgia Tech for graduate school. He has also provided constructive advice developing future research goals and "selling my thesis".

Everyone is the Wood and Jang lab has provided a nurturing environment for my educational and professional growth. I would especially like to thank fellow graduate students that have worked in the Wood lab: Michael Griffin, Laura Weinstock, Sitara Sankar and Alyssa Pybus for helping to develop a working environment that is friendly,

supportive and family-like at times, in which I have thrived and developed as a person and scientist beyond anything I thought possible. I am also thankful for the opportunity to guide devoted undergraduate students Aditya Datye and Andrew Hong, both of whom have continued their educational and research based development in other labs.

Lastly, I would like to thank my parents Ruth and Steve Long, my aunt Rebecca DeBolt and godfather Ron Cates for continually pushing me to reach for new goals. They have all challenged me to become a better person and motivated me to develop my education. I would also like to thank my late grandmother Joan Long for heavily influencing my interest in the medical field, without which I would not be graduating from Georgia Tech. Ron also deserves thanks for encouraging me to pursue difficult yet worthwhile education. Rebecca helped me during my time in Akron and showed support and advice as I was developing into a proper adult. My parents notably deserve the most thanks for supporting every decision that I have made, ranging from which sports I wanted to play as a kid all the way to choosing to attend graduate school at Georgia Tech.

In short I am incredibly grateful for all the people that have enriched my life.

TABLE OF CONTENTS

ACKNOWLEDGEMENTS iii

LIST OF TABLES vi

LIST OF FIGURES vii

LIST OF SYMBOLS AND ABBREVIATIONS xi

SUMMARY xii

CHAPTER 1. Introduction 1
1.1 Alzheimer's Disease 1
1.2 A Need to Look Beyond Amyloid Beta 2
1.3 Blood Brain Barrier Breakdown 4
1.3.1 Structure and Function 4
1.3.2 Vascular Dysfunction 4
1.4 Junction Proteins 5
1.4.1 Function and Regulation 5
1.4.2 VE-Cadherin and Platelet Endothelial Cell Adhesion Molecule 7
1.5 Alzheimer's Disease Microenvironment 8
1.6 Contributions of this Thesis 8

CHAPTER 2. "Charting" Endothelial cell function, protein expression and signaling 14
2.1 Designing an Array of Experiments to Probe Endothelial Cell Function 14
2.2 Choosing a Concentration of Aβ for Experimental Design 17
2.3 Preliminary Immunocytochemistry 18
2.4 Dextran Diffusion in Aβ and Inflammatory Conditions 21
2.5 Quantification of Barrier Function 26
2.6 Reduced Angiogenic Growth in Aβ Conditions 29
2.7 Upregulated MAPK Signaling in Aβ and Pro-Inflammatory Conditions 32

CHAPTER 3. Conclusion 38
3.1 Contributions of This Work 38
3.2 Future Directions 39

APPENDIX A. Materials and Methods 41
A.1 Device Fabrication 41
A.2 Cell Culture 42
A.3 Dextran Permeability 44
A.4 Junction Protein Quantification 45
A.5 Angiogenic Growth Measurement 48
A.6 Phosphorylated Protein Analysis 50

LIST OF TABLES

Table 1 - Mixing ratios for creating common western blotting buffers. Reagents for creating buffers include trizma base (Sigma Aldrich – Cat No. T1503-5KG), glycine (Alpha Aesar – Cat No. J64365-A1), 20% SDS (Sigma Aldrich – Cat No. 05030-500ML-F) and NaCl (Aldon Corp SE – Cat No. SS0450-500G). 46

LIST OF FIGURES

Figure 1	- Illustration of BBB leakiness. A permeable capillary will allow red blood cells and peripheral immune cells to leak into the brain interstitial space.	6
Figure 2	- Illustration of cell-cell adhesion. Junction proteins allow for cells to adhere to each other.	7
Figure 3	- A growth region where endothelial cells have adhered to the protein scaffold to form an endothelial cell monolayer	9
Figure 4	- Representation of how endothelial cell intracellular signaling can regulate multiple functions of the BBB.	10
Figure 5	- Experimental layout of the microfluidic device and how dextran will diffuse through the gel region. Characterization of diffusion requires an intact endothelial cell monolayer across the entire device to be quantified.	11
Figure 6	- Demonstration of our ability to grow and identify the 3D endothelial monolayer that is to be quantified for protein expression. Red: PECAM, Green: VE-Cadherin, Blue: Dapi. Endothelial cells grow along the top and bottom of the channel as well as against the protein scaffold. The highlighted wall is a growth region as previously illustrated in figure 3.	12
Figure 7	- Technique of how to identify angiogenic sprouts. Cells must be attached to count as a branch. Detached cells do not actually form angiogenic sprouts. Distances that sprouts grew into the gel region were quantified with identifying sprouts in this manner. Timepoints of 0 hour (before angiogenesis) and 48 hour (after angiogenesis) were taken to measure distance travelled during conditioning.	13
Figure 8	- Western blot analysis of hMVEC dose-response to Aβ. (A) Western blot showing PECAM, VE-Cadherin and α-tubulin expression of hMVEC 6-well plate cultures in control and Aβ concentrations ranging 100nM-500nM. (B) Fluorescent intensity values normalized to first α-tubulin intensity then controls. Significant reduction in protein expression were found in PECAM experiments at 400nM ($p = 0.026$) and 500nM ($p < 0.0001$) and in VE-Cadherin experiments at 500nM ($p = 0.0071$).	18

Figure 9 - Immunofluorescent staining for adheren junction proteins in hMVECs growing in 2.5mg/mL collagen and 3mg/mL Matrigel 1:1 mixture. Blue: Dapi. Red: Phalloidin. Green: VE-Cadherin. Purple: PECAM. Cells were grown for 7 days to ensure monolayer formation on all surfaces. Conditions were Control, 50nM Aβ, 50ng/mL VEGF, 20ng/mL TNF-α, 50nM Aβ + 50ng/mL VEGF and 50nM Aβ + 20ng/mL TNF-α and show respective junction protein expressions. Images are maximum intensity projections of the 3D microenvironment. 19

Figure 10 - Immunofluorescent images demonstrating a clear 3D growth pattern where hMVECs form a monolayer on the top, bottom and posts of the device. Blue: Dapi. Red: Phalloidin. Green: VE-Cadherin. Purple: PECAM. (A) Isometric view of 3D microenvironment within the device. (B) Side view demonstrating cells grow to form monolayers on top, bottom and on posts while leaving an opening in between the surfaces to generate vessel-like constructs. 22

Figure 11 - Dextran Diffusion shows endothelial cell monolayer permeability in response to inflammatory cytokines and Aβ in transwell plates. Fluorescent intensity of diffused dextran in various conditions with background subtracted and normalized to controls. Bars represent standard error of the mean with a significant difference established between Control and every other condition ($p<0.05$) using one-way ANOVA and Brown-Forsythe post hoc tests. 24

Figure 12 - Dextran Diffusion shows endothelial cell monolayer permeability in both transwell plates and microfluidic devices. (A) Fluorescent images of diffused dextran in various conditions. (B) Fluorescent intensity quantification showing diffusion through endothelial cell monolayer into the collagen gel region in microfluidic devices. Bars represent standard error of the mean and no statistical significance was established ($n = 4$). 25

Figure 13 - Western blot analysis shows endothelial cell monolayer protein expression in 6-well plate cultures. (A) Membranes, fluorescently imaged with Li-Cor imaging system, show protein expression with respect to conditions and loading controls. (B) Quantification of PECAM protein expression in response to the various conditions: Vehicle, 300nM Aβ, 50ng/mL VEGF, 20ng/mL TNF-α, 300nM Aβ+50ng/mL VEGF and 300nM Aβ+20ng/mL TNF-α shows a trend where all conditions downregulate protein expression, however, no statistical significance was established. (C) Quantification of VE-Cad protein expression shows similar trend 27

to PECAM also with no statistical significance established (n = 4 for all).

Figure 14 - Quantification of barrier function using fluorescent intensity of a 3D monolayer grown against the collagen scaffold. (A) Representative images showing monolayer against the protein scaffold quantified for each condition. Images are maximum intensity projections of the 3D microenvironment. (B) Images depict sections demonstrating front views of 3D rendered devices from images in part A. (C) Quantification of barrier proteins were normalized to cell count and demonstrates statistically significant downregulated PECAM expression in response to Aβ ($p = 0.007$), but not other conditions (n = 3). (D) VE-Cad quantification shows no significant changes in protein expression or a trend (n = 3). 28

Figure 15 - Phase contrast and live cell fluorescent imaging for tracking angiogenic sprouting of hMVECs grown in 2.5 mg/ml collagen gel at 0 and 48 hours for Control and VEGF stimulated conditions. Graphics demonstrate the method used to quantify the distances of angiogenic sprouting. 30

Figure 16 - Quantification of angiogenic growth, as measured with the technique shown in figure 15, demonstrates Aβ decreases angiogenic sprouting distances into the gel region with respect to both Control and VEGF conditions. Statistical significance was established between control and Aβ ($p = 0.005$), VEGF and Aβ+VEGF ($p = 0.037$), and control and Aβ+VEGF ($p = 0.023$) with (n = 105 growth regions from 3 devices) using one-way ANOVA and post hoc tests. 31

Figure 17 – MAPK intracellular signaling pathway in the context of VEGF and TNF-α receptor activation. 32

Figure 18 - Partial least squares regression of intracellular signaling MAPK readings. (A) Heatmap shows intensity of phosphorylated MAPK protein expression in harvested cells lysates in 4 conditions: Control, 50nM Aβ, 50ng/mL VEGF and 50nM Aβ + 50ng/mL VEGF. (B) Partial least squares discriminate analysis of the 4 conditions shows separation of conditions along latent variables (LVs) 1 and 2. (C-D) Latent variables were calculated and show protein expression that are upregulated or downregulated with respect to z-score of conditions along each latent variable as shown in part (B). 34

Figure 19 - Partial least squares regression of intracellular signaling MAPK readings. (A) Heatmap shows intensity of phosphorylated MAPK protein expression in harvested cells lysates in 4 conditions: 35

Control, 50nM Aβ, 50ng/mL VEGF and 50nM Aβ + 50ng/mL VEGF. (B) Partial least squares discriminate analysis of the 4 conditions shows separation of conditions along latent variables. (C-D) Latent variables were calculated and show protein expression that are upregulated or downregulated with respect to z-score of conditions along each latent variable as shown in part (B).

Figure 20 - Partial least squares regression of intracellular signaling MAPK readings. (A) Heatmap shows intensity of phosphorylated MAPK protein expression in harvested cells lysates in 4 conditions: Control, 50nM Aβ, 50ng/mL VEGF and 50nM Aβ + 50ng/mL VEGF. (B) Partial least squares discriminate analysis of the 4 conditions shows separation of conditions along latent variables. (C-D) Latent variables were calculated and show protein expression that are upregulated or downregulated with respect to z-score of conditions along each latent variable as shown in part (B). 36

Figure 21 - Setup of various steps within device fabrication. Devices remain in a pseudo-sterile environment after autoclaving and maintain sterility during PDL treatment and cell culturing. 41

Figure 22 – Demonstration of the technique for cell seeding into devices 44

Figure 23 - Approximate regions for fluorescent intensity readings for dextran diffusion. 45

Figure 24 - Highlights the approximate areas where endothelial cells interact with the collagen protein matrix and form a monolayer for quantification. 48

Figure 25 - (A) Table showing conditioning strategy for both channels in the angiogenesis assay. (B) Demonstration of pipetting strategy for maintaining pressure equilibrium during conditioning. 49

LIST OF SYMBOLS AND ABBREVIATIONS

AD	Alzheimer's Disease
Aβ	Amyloid Beta
BBB	Blood Brain Barrier
VEGF	Vascular Endothelial Growth Factor
TNF-α	Tumor Necrosis Factor alpha
PECAM	Platelet Endothelial Cell Adhesion Molecule
VE-Cadherin	Vascular Endothelial Cadherin
MRI	Magnetic Resonance Imaging
CAA	Cerebral Amyloid Angiopathy
TJ	Tight Junction
AJ	Adheren Junction
GJ	Gap Junction
MAPK	Mitogen Activated Protein Kinase
ELISA	Enzyme-Linked Immunosorbent Assay
PDMS	Poly-dimethylsiloxane
HSP	Heat Shock Protein
ERK	Extracellular signal-regulated kinase
PLSR	Partial Least Squares Regression
PLSDA	Partial Least Squares Discriminant Analysis

SUMMARY

Alzheimer's disease (AD) is the most common form of dementia, affecting more than 35 million people worldwide, and lacks any effective therapy to stop or slow the disease. AD is characterized by progressive appearance of extracellular amyloid beta (Aβ) plaques in affected regions of the brain, which lead to neuronal dystrophy and death. There is increasing evidence, however, that Aβ is not the sole driver of disease progression. A functional MRI study has revealed that the blood-brain barrier (BBB), a vital regulator of molecular transport between the brain and vascular system comprised in part of microvascular endothelial cells, becomes leaky early in disease. Furthermore, analysis of postmortem tissue has revealed reduced angiogenic vascular growth in AD tissues. Thus, vascular defects may promote neuronal death by reducing perfusion and allowing peripheral cells to enter the brain. The mechanisms responsible for BBB breakdown have not been delineated, but may be influenced or driven by Aβ and neuroinflammation. Inflammatory cytokines such as tumor necrosis factor alpha (TNF-α) have been previously established by our lab and others to be upregulated in the AD microenvironment. I hypothesize that Aβ and inflammatory cytokines together drive loss of vascular endothelial barrier function and angiogenic sprouting. To test this hypothesis, I have used an integrated cell culture approach combining transwell plates, 2D cell cultures, and 3D microfluidic devices. Dextran permeability assays in microfluidics and transwell plates demonstrate that Aβ conditions increase endothelial permeability. Further, western blotting of 2D cultures demonstrates a dose-dependent down-regulation of both platelet-endothelial cell adhesion molecule (PECAM) and VE-cadherin expression in response to Aβ. Since PECAM is a

critical regulator of angiogenesis, I quantified changes in angiogenic sprouting in response to Aβ using our microfluidic platform, thus in total my data will link PECAM dysregulation to dual vascular pathologies in AD: loss of barrier function and reduced angiogenic growth. In total, my data demonstrate that Aβ and key AD cytokines effect endothelial barrier function and angiogenic sprouting. Moreover, my approach combining 2D and physiologically relevant 3D cell cultures provides great utility for interrogating vascular response to specific components of the AD microenvironment.

CHAPTER 1. INTRODUCTION

1.1 Alzheimer's Disease

Alzheimer's disease (AD) is the most common form of dementia, affecting more than 35 million people worldwide [1]. AD clinical symptoms begin with memory loss and progress to include changes in behavior, decline of motor control, loss of language and eventual death [1]. No effective therapies have been found to stop or slow disease progression. The primary risk factor for AD is age, which stresses the importance for developing effective therapies considering the aging worldwide population [1]. In AD, amyloid beta (Aβ) aggregates in the brain, forming plaques and leading to tissue aberrations that can cause neuronal death [1]. Traditional efforts have focused on preventing this protein aggregation, however, recent clinical trials targeting Aβ formation have not been able to stop or slow disease progression [2], which suggests Aβ aggregation is not the sole driver of the disease. In AD, protein aggregation is accompanied by neuroinflammation and vascular dysfunction, two factors that can drastically influence the brain microenvironment [3, 4]. Vascular dysfunction, in particular, allows neurotoxic molecules and peripheral immune cells into the brain [4], which can further promote neuroinflammation and production of neurotoxic molecules [5]. Thus, a strategy to restore vascular homeostasis, may be effective to stop or slow disease progression. Vascular function is heavily influenced by endothelial cells that form blood vessels. Therefore, the objective of this thesis is to understand how Aβ and neuroinflammation affect microvascular endothelial cell function and how Aβ and neuroinflammation relate to vascular dysfunction in AD.

1.2 A Need to Look Beyond Amyloid Beta

AD is characterized by the progressive appearance of extracellular amyloid beta (Aβ) plaques in affected brain regions [6]. Aβ is created by cleavage of amyloid precursor protein (APP) by first β-secretase then γ-secretase, thus releasing Aβ monomers into the extra-cellular compartment to aggregate and form Aβ plaques [6]. These plaques aggregate in extracellular sites that are affected by AD and consequently have been shown to stimulate neuropathology [7]. Though Aβ is a pathological marker of AD, recent clinical trials targeting Aβ as a therapeutic strategy have not been able to establish a working therapy. For example, trials targeting Aβ with a γ-secretase inhibitor resulted in accelerated disease progression rather than preventing disease progression [2, 8]. Furthermore, trials targeting Aβ for clearance using anti-Aβ monoclonal antibodies demonstrated reduced Aβ, but did not show significant cognitive improvement [2, 8]. More recently, trials using a β-secretase inhibitor were stopped due to patients having continued cognitive decline and showing no measurable preventative effects for pathological progression of AD [8]. State-of-the-art technology for Aβ clearance is Biogen's new antibody, aducanumab, which reduces Aβ in the AD microenvironment [9]. Aducanumab has just finished phase II trials and is currently in phase III trials [9]. Considering the outcomes of these clinical trials and lack of positive results in gamma secretase inhibitor, beta secretase inhibitor and previous anti-amyloid antibody phase III trials, Aβ is not likely the sole driver of disease progression.

Looking beyond Aβ, there are other classic pathologies observed in AD. In addition to Aβ plaques formation, tau protein within neurons becomes hyper-phosphorylated and forms intracellular neurofibrillary tangles which have traditionally been thought to aid in

neuronal death [7]. Other changes in the AD microenvironment involve an upregulation of oxidative stress, upregulation of neuroinflammation and vascular dysfunction [10]. Increased oxidative stress is characterized by highly reactive superoxide molecules that lead to increased cytotoxicity and cell death [11]. Neuroinflammation is a result of glial activation, where microglia and astrocytes secrete pro-inflammatory cytokines, a process that becomes dysregulated in AD [10]. Lastly, vascular dysfunction is characterized by plasma proteins and circulating peripheral immune cells leaking into the AD microenvironment [12]. Though multiple pathologies are observed in AD, this thesis focuses primarily on dysregulated cytokine levels from neuroinflammation and vascular dysfunction as seen in AD.

Looking at vascular dysfunction, functional MRI studies have demonstrated vascular leakiness early in AD [13]. This blood brain barrier (BBB) dysregulation is possibly due to Aβ or upregulated inflammatory cytokines. Further studies have shown in humans and AD transgenic mice, that Aβ co-localizes on capillaries which is correlated with cerebral amyloid angiopathy (CAA), possibly inducing endothelial cell response that affects BBB integrity [14]. CAA is a potential contributor to Aβ co-localization around blood vessels in the brain, possibly leading to increased levels of Aβ as seen by endothelial cells and in turn enhancing vascular dysfunction as seen in AD [15, 16]. However, AD model mice do not experience the complete vascular dysfunction observed in humans [17], providing difficulty in quantifying vascular changes due to Aβ co-localization. Additionally, Neuorinflammation has been shown to be induced by Aβ aggregation [14]. Furthermore, human AD brain tissue studies have shown upregulation of pro-inflammatory cytokines in AD tissues, likely caused by neuroinflammation [4]. This is possibly leading

to endothelial cell functional changes or even apoptosis, causing vascular dysfunction in AD. Therefore, studying the BBB and how it becomes dysfunctional in response to Aβ is likely to yield new insight for developing a therapeutic strategy for preventing or slowing disease progression.

1.3 Blood Brain Barrier Breakdown

1.3.1 Structure and Function

The BBB is a vital regulator of molecular transport between the brain and vascular system, which is comprised of complex capillary networks that include endothelial cells, pericytes and astrocytes [18, 19]. Endothelial cells are of particular interest because they act as the primary structural component of the BBB, expressing cell-cell junction proteins that are responsible for maintaining endothelial barriers [20, 21]. During tissue homeostasis, the BBB is effective at preventing neurotoxic pathogens and peripheral immune cells from entering the brain as well as allowing passage of water, glucose and amino acids [18, 22, 23].

1.3.2 Vascular Dysfunction

Though the BBB acts as a potent barrier against neurotoxic pathogens and peripheral immune cells during tissue homeostasis, most AD patients show vascular leakiness early during disease progression [12, 24]. Postmortem AD tissues show vascular leakiness as well, which suggests vascular defects may contribute to disease progression by reducing perfusion and allowing peripheral immune cells to enter the brain which could promote neuronal death [25]. Vascular defects can be divided into two major categories: 1)

dysregulated angiogenesis and 2) reduced barrier function. Angiogenesis is the main function by which endothelial cells create new vasculature [26-28]. Angiogenesis is characterized by endothelial cell invasion into extracellular matrix led by a tip cell where migration can be driven by growth factor concentration gradients [26, 27]. This mechanism creates the foundation for new capillaries within the brain and is dysregulated in AD as demonstrated by reports of AD tissues with reduced angiogenic vascular growth [29, 30]. Barrier function is tightly regulated by cell-cell junction proteins such as VE-Cadherin (VE-Cad) and zonula occludin 1 (ZO-1) in endothelial cells during tissue homeostasis, but becomes dysfunctionally regulated in tissues affected by Alzheimer's pathology [12, 14, 31, 32]. Reduced expression of junction proteins such as VE-Cad or platelet endothelial cell adhesion molecule (PECAM) is known to lead to increased vascular permeability or reduced angiogenic growth [24, 31, 33-35]. Thus, dysregulated PECAM and VE-Cad protein expression possibly affect the BBB by preventing vessel repair/regrowth and causing leaky vessels, an example of which can be seen in figure 1, respectively in AD [14]. Concurrently, some junction proteins are able to regulate angiogenesis [36], therefore junction proteins have significant angiogenic stimuli that are critical for elucidating disease progression.

1.4 Junction Proteins

1.4.1 Function and Regulation

Endothelial cells have high expression of junction proteins in the brain microenvironment, which can be divided into three groups: tight junctions (TJs), adheren junctions (AJs) and gap junctions (GJs) [37]. TJs prevent molecular and electrical transport [24]. AJs primarily

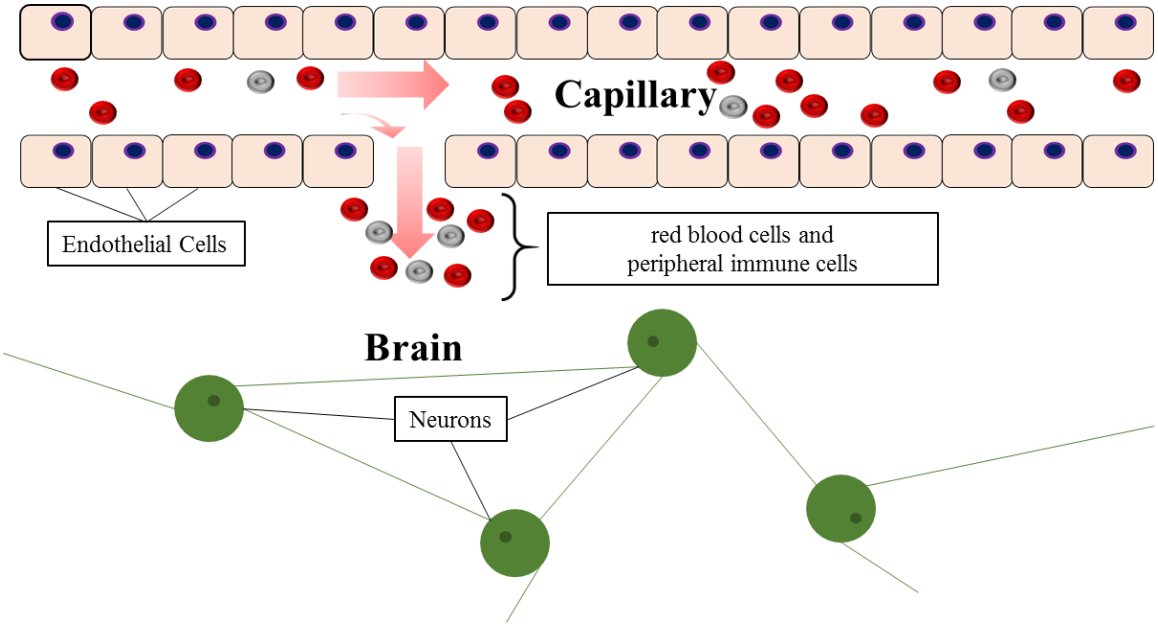

Figure 1 - Illustration of BBB leakiness. A permeable capillary will allow red blood cells and peripheral immune cells to leak into the brain interstitial space.

provide structural support to adjacent cells, illustrated in figure 2, and propagate downstream intracellular signaling based on structural and extracellular biochemical influences [31, 32]. GJs are selective to cell-cell passage of proteins and electrical signals, therefore allowing direct signal transduction from cell to cell [38]. Though all three types of junction proteins are highly expressed and play an important role in maintaining BBB integrity, AJs play a unique role in modulating various endothelial cell functions [31, 32, 39]. Several intracellular signaling pathways such as mitogen activated protein kinase (MAPK) pathways are stimulated upon AJ inhibition or activation which can lead to angiogenesis or barrier enhancement respectively [40, 41]. A recent study demonstrated that Aβ downregulates expression of the TJ claudin 5, which suggests that Aβ affects barrier function [42]. Since several barrier promoting-signaling pathways that promote claudin 5 expression are mediated by AJ activation, we can conclude that Aβ downregulates AJ signaling [31, 43]. Two notable AJs that are potent regulators of barrier

function and angiogenesis modulation in endothelial cells are PECAM and VE-Cadherin [31, 36]. These proteins are ubiquitously expressed in endothelial cells in the BBB and have not been previously linked to Aβ. Therefore, probing the effects of Aβ or inflammatory cytokines on these proteins will provide new insight into mechanisms driving dysregulation of the BBB in AD.

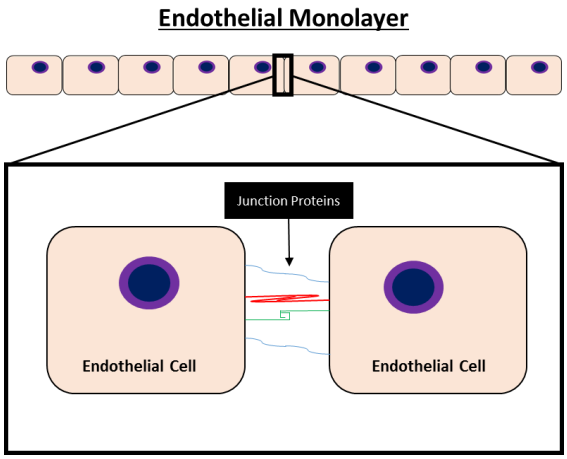

Figure 2 - Illustration of cell-cell adhesion. Junction proteins allow for cells to adhere to each other.

1.4.2 VE-Cadherin and Platelet Endothelial Cell Adhesion Molecule

PECAM and VE-Cadherin are both highly expressed in brain microvascular endothelial cells with the primary function of maintaining cell-cell adhesion or regulating angiogenesis [31, 35, 36]. VE-Cadherin is established as a potent driver of cell-cell adhesion and has also been shown to play a vital role in maintaining newly formed vessels [31]. VE-Cadherin can be stimulated via angiopoietin to increase VE-Cadherin expression or vascular endothelial growth factor (VEGF) to reduce VE-Cadherin expression [39]. PECAM primarily acts as a cell-cell adhesion protein, but can also internalize to phosphorylate proteins for modulating downstream angiogenic signaling via the MAPK pathway [34, 36].

Downregulation of both these functions suggests PECAM expression is reduced in AD, leading to the reduced angiogenic vascular growth, as reported in postmortem AD tissues [24].

1.5 Alzheimer's Disease Microenvironment

Analysis of postmortem AD tissues has established that numerous pro-inflammatory cytokines are upregulated in AD [5, 44, 45]. Several of these cytokines are known to dysregulate endothelial function [5], suggesting that neuroinflammation has a large impact on endothelial cell junction protein expression. Astrocytes, upon activation, secrete inflammatory cytokines such as VEGF or tumor necrosis factor alpha (TNF-α), both of which can decrease junction protein expression [45]. Other upregulated cytokines in the AD microenvironment have been reported to increase the production of Aβ, thereby increasing plaque deposition [45]. Though inflammation can be a normal part of healing and secreted growth factors are necessary for cell growth [5, 44], dysregulation of cytokine expression in AD affects junction protein expression and Aβ aggregation, promoting disease progression [4, 14].

1.6 Contributions of this Thesis

There is a clear clinical need for understanding the driving mechanisms that lead to vascular dysfunction in Alzheimer's pathology. Since Aβ-focused strategies have not restored cognitive function, AD research approaches should broaden the scope to further understand the role that endothelial cells play as a regulator of BBB function in AD. The lack of knowledge base in this particular research field requires identification of core mechanisms driving vascular dysfunction in AD. In this thesis, I advanced understanding of how Aβ

and neuroinflammatory factors affect endothelial cell function which will be an essential step in vascular dysfunction research in the context of AD.

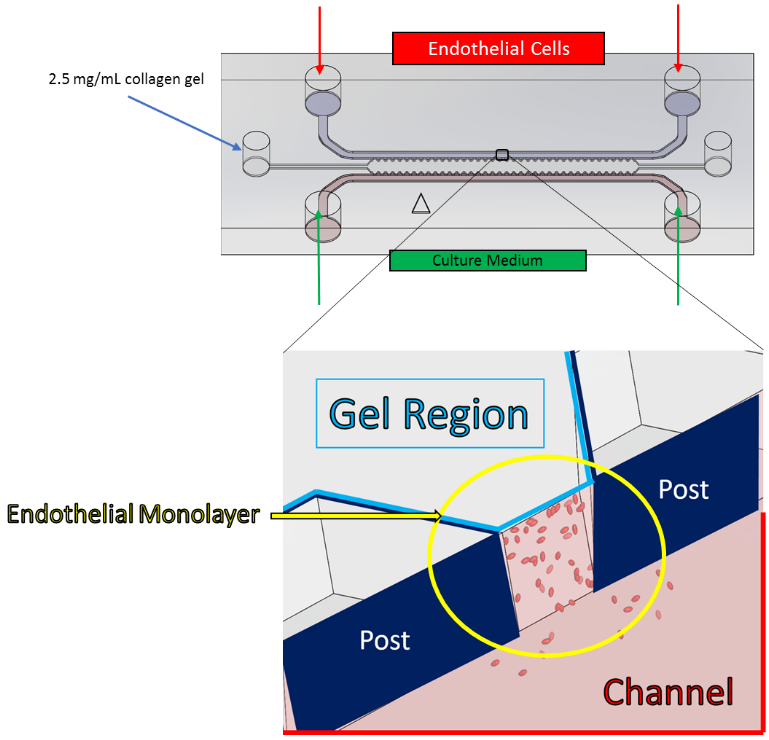

Figure 3 - A growth region where endothelial cells have adhered to the protein scaffold to form an endothelial cell monolayer in a microfluidic chamber.

In this thesis, I take the first step toward establishing culture and function measuring methods by utilizing a 3D microfluidic culture platform, illustrated in figure 3, to identify a core signaling pathway dysregulated in endothelial cells as a response to two cytokines upregulated in AD: VEGF and TNF-α. I use several common biological tools such as immunocytochemistry, western blots, dextran diffusion, ELISA and an angiogenesis assay that has been previously established [46]. Since endothelial cells play a central role in maintaining BBB function, we are interested in delineating specifically how endothelial cells are affected by the AD microenvironment.

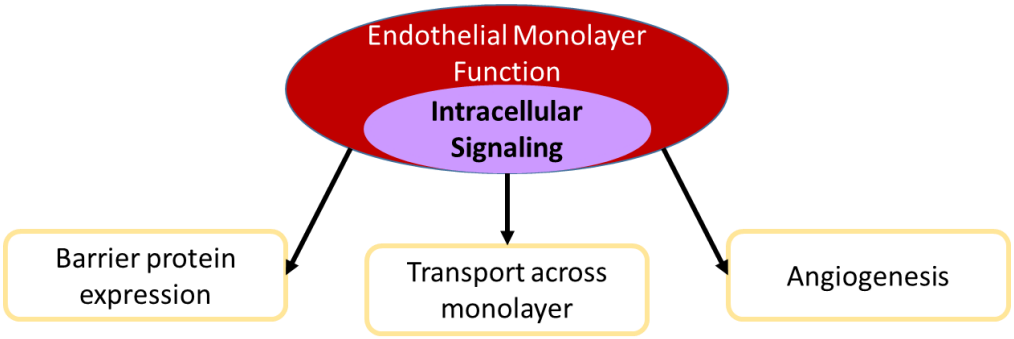

Figure 4 - Representation of how endothelial cell intracellular signaling can regulate multiple functions of the BBB.

In the following chapters, I take the following approach (conceptual illustration in figure 4) to identify a core signaling mechanism that is dysregulated in response to VEGF or TNF-α:

- **Functional assay quantification** Establish reproducibility with an existing microfluidic assay that was previously designed [46] to probe changes in endothelial barrier functions in response to Aβ, TNF- α and VEGF. An endothelial cell monolayer forms along a protein scaffold with several scaffold-exposed growth regions. Quantification of barrier function was measured via transport across a monolayer.

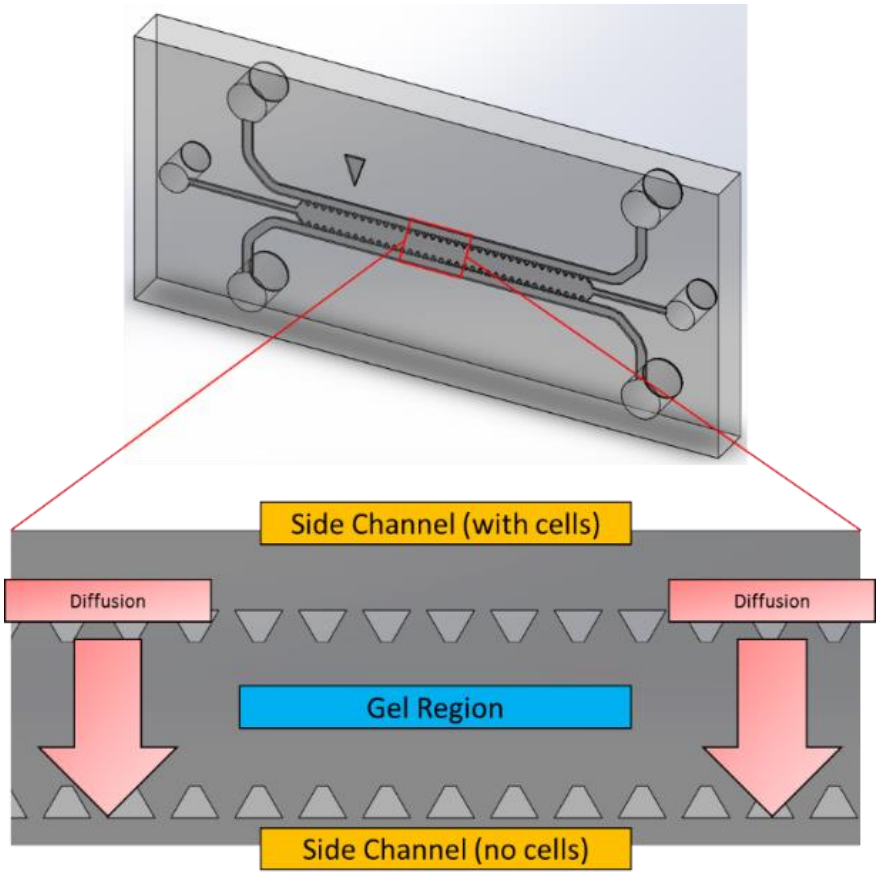

Figure 5 - Experimental layout of the microfluidic device and how dextran will diffuse through the gel region. Characterization of diffusion requires an intact endothelial cell monolayer across the entire device to be quantified.

- **Adheren Junction protein expression** Demonstrate differences in adheren junction protein expression in response to the various conditions including: Control, VEGF, TNF-α or Aβ. This will verify endothelial cell-cell adhesion protein expression and demonstrate clear structural differences in response to inflammatory and pathological AD biochemical stimuli.

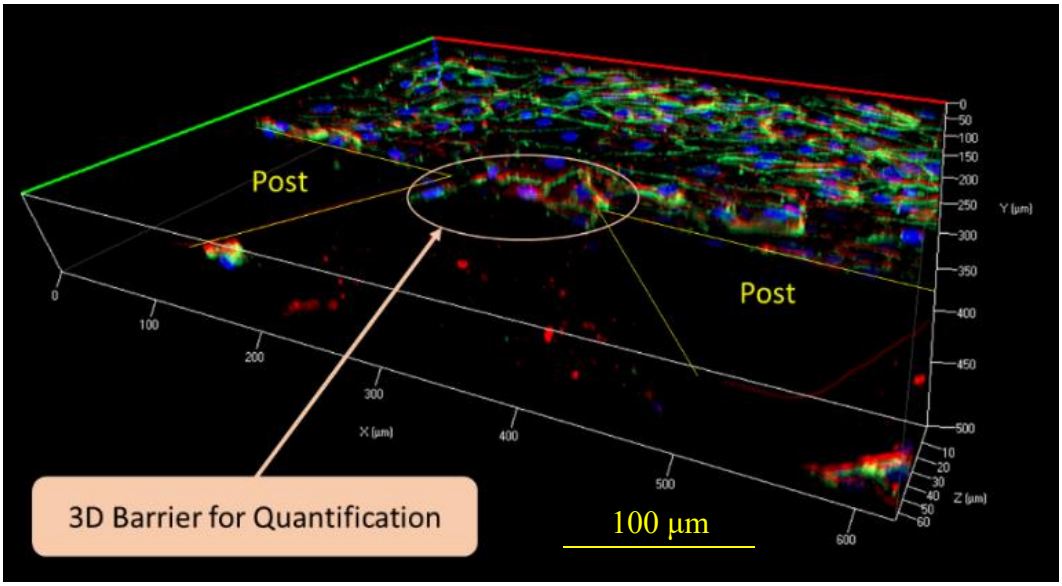

Figure 6 - Demonstration of our ability to grow and identify the 3D endothelial monolayer that is to be quantified for protein expression. Red: PECAM, Green: VE-Cadherin, Blue: Dapi. Endothelial cells grow along the top and bottom of the channel as well as against the protein scaffold. The highlighted wall is a growth region as previously illustrated in figure 3.

- **Angiogenesis quantification** Employ an assay previously developed to characterize nascent vessel formation and elongation in response to VEGF and Aβ. Angiogenesis can then be quantified by the length of angiogenic sprouts growing from the side channel towards a VEGF gradient using CMFDA live cell tracking, bright field and Hoechst with which to image.
- **MAPK intracellular analysis** Identify MAPK signaling pathways that are upregulated in endothelial cells as a response to inflammatory cytokines and Aβ. This can help determine targets to inhibit which would ideally reverse signaling pathway upregulation, therefore, restoring homeostasis.

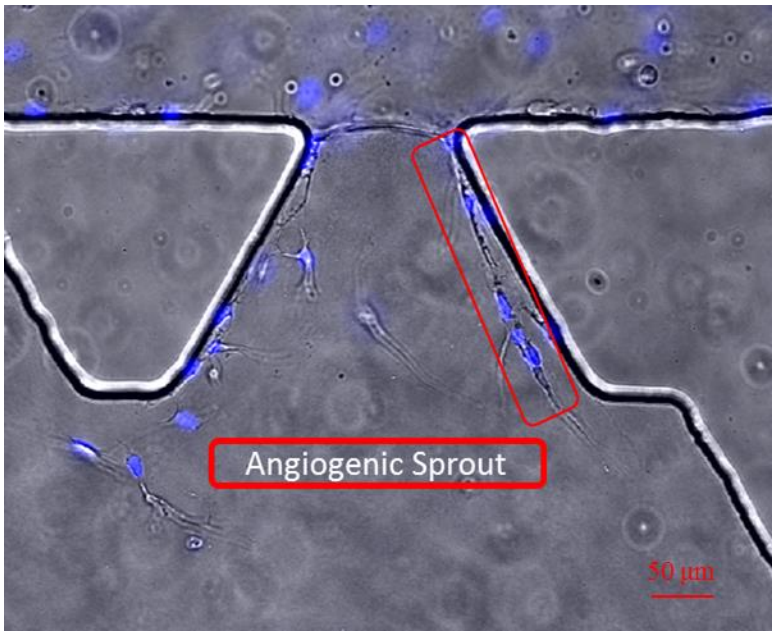

Figure 7 - Technique of how to identify angiogenic sprouts. Cells must be attached to count as a branch. Detached cells do not actually form angiogenic sprouts. Distances that sprouts grew into the gel region were quantified with identifying sprouts in this manner. Timepoints of 0 hour (before angiogenesis) and 48 hour (after angiogenesis) were taken to measure distance travelled during conditioning.

Collectively, this thesis utilizes an array of methodologies for characterizing several domains of endothelial cell function in conjunction with an innovative 3D microvascular culture platform to probe endothelial cells with Aβ and cytokines that negatively affect the BBB. Utilizing this method, we found: 1) increased permeability in response to Aβ and cytokines, 2) junction protein expression is reduced in response to Aβ and cytokines, 3) Aβ causes reduced angiogenic growth, and 4) p38 MAPK signaling is upregulated in response to Aβ and VEGF.

CHAPTER 2. "CHARTING" ENDOTHELIAL CELL FUNCTION, PROTEIN EXPRESSION AND SIGNALING

2.1 Designing an Array of Experiments to Probe Endothelial Cell Function

Endothelial cell function may be quantified in terms of four primary readouts [20, 47-49]:

- Endothelial monolayer permeability
- Barrier protein expression
- Angiogenesis
- Intracellular signaling

In vivo experiments are regarded as the most physiologically relevant study for AD research [50, 51]. Because *in vivo* experiments in humans would be unethical, mice are commonly used for AD research due to their short lifespan and a need for aged test subjects. However, mice do not naturally suffer from dementia, therefore transgenic mice are required for AD research [50, 51]. And although mice have short lifespans, aging mice takes 1-2 years to prepare for AD studies, slowing the progress of research in this field [50, 51]. Also, perturbation of the mouse brain microenvironment elicits responses across several cell types and tissues, leading to difficulty in isolating changes from a single cell type. *In vitro* cultures on the other hand provide an environment where specific changes in endothelial cells can be easily measured. Because of the time scale of AD research and difficulty in interrogating endothelial cell specific responses *in vivo*, we decided to utilize only *in vitro* methods for measuring changes in endothelial cell function in response to Aβ, TNF- α and VEGF.

Current methods for analyzing endothelial monolayer integrity include: transwell plates, Matrigel cell cultures, spheroidal cultures, microfluidic platforms and *in vivo* studies [19, 50, 52].

Transwell plates have strong potential for measuring biochemical interactions between cells and have proven to be powerful for characterizing the diffusion of drugs through the BBB *in vitro* [53]. Several studies have also utilized transwell plates to measure the diffusion of FITC Dextran which depending on the size of the dextran, can show permeability of endothelial monolayers in response to biochemical stimuli [42, 53, 54]. Considering the benefits of this culture platform, transwell plates were an excellent method for measuring the diffusion of dextran through an endothelial monolayer in response to Aβ, TNF- α and VEGF. One way to enhance physiologic relevance of transwell plates is to seed a protein matrix of Matrigel or collagen gel on which the endothelial cells can grow into each well.

Matrigel is a protein matrix that is comprised of primarily laminin, hyaluronic acid and type IV collagen, which provide a highly physiologic protein matrix for brain extracellular matrix [53, 55]. Many studies have demonstrated the utility of Matrigel when culturing neurons, microglia, endothelial cells and other components of the brain [55]. Therefore, BBB studies often use Matrigel as their protein matrix with which cell-cell interaction among endothelial cells, astrocytes and pericytes is enabled [53, 55]. The effective use of Matrigel is dependent on the experimental design in which it is employed, such as the now common microfluidic BBB on a chip model [19, 56]. Though there is physiologic relevance in Matrigel, problems with endothelial cell invasion into the matrix provided difficulties in forming endothelial monolayers, arguably a more important aspect

of physiologic relevance of endothelial cell cultures [57]. This was likely due to the fact we were using growth factor rich Matrigel, leading to a chemotactic response in endothelial cells to grow into the matrix. Therefore, we decided to use collagen gel due to improved efficacy in growing endothelial monolayers [58].

Spheroids are self-assembling constructs that include endothelial cells, astrocytes and pericytes in the shape of a sphere [53]. This culture method is great at monitoring cellular interaction due to cells in physical contact with one another [53]. However, the spheroid does not form an endothelial monolayer that could be used to quantify endothelial cell function, therefore, we decided not to use this culture method for characterizing changes in endothelial cell function in response to Aβ, TNF- α and VEGF.

Microfluidic culture platforms are highly physiologic with the ability to accurately model the cellular microenvironment [19, 56]. Several labs focus on designing new innovative platforms to increase physiologic relevance of *in vitro* studies with respect to various tissues [19, 59, 60]. For example, microfluidic platforms are often used for multicellular cultures, including BBB studies which have complex systems such as electrical stimuli mimicking a brain-like microenvironment or multiple layers to accurately portray layers of cells [19]. Though these systems are highly physiologic, our primary interest is specifically understanding endothelial cell response, therefore, we cultured endothelial cells to form an endothelial monolayer against a protein matrix to mimic a micro vessel. Considering our needs, we decided to use a microfluidic platform that could sustain a protein matrix with side channels, a simplified version of the more complex systems mentioned above [46].

Several previous studies in interrogating endothelial function in the context of BBB function have used cell lines, particularly for brain endothelial cells, the HCMEC/D3 cell line [42, 56, 61]. Previously mentioned TJ studies were conducted using these cells to show reduced claudin 5 protein expression [42], however, cell lines are commonly regarded as less physiologic than primary cells due to genetic mutations that allow continuous use [56]. In order to enhance physiologic relevance, we decided to use human microvascular endothelial cells (hMVECs – detailed in the Appendix). Though these cells are harvested from human skin instead of the brain, they are still arguably more physiologically relevant than a genetically mutated cell line [56]. We primarily chose to use hMVECs because of prior studies utilizing our device design and hMVECs to interrogate changes in angiogenic growth, a metric we aim to measure [46]. Though these are not brain derived endothelial cells, we will establish baseline readings with which to compare to brain endothelial cells in future studies.

2.2 Choosing a Concentration of Aβ for Experimental Design

To characterize cellular changes during AD in response to Aβ, concentrations close to physiologic ranges should be used. Traditionally, studies probing cellular response to varying concentrations of Aβ (1-10μM) [42] have reached orders of magnitude higher than recorded physiologic ranges (5-500nM) [62, 63]. In order to characterize cell response to a more physiologic concentration of Aβ than previous studies, we conducted a dose response experiment to identify a dosage for decreased junction protein expression. Endothelial cells have a clear dose response to Aβ which was characterized via western blots and can be seen in figure 8 which utilized protocols detailed in the Appendix A.4.1. PECAM expression significantly decreases at concentrations of Aβ reaching 400 and 500

nM. However, we chose to use 300nM of Aβ for our experimental setup because we wanted to be able to identify combined effects of Aβ with neuroinflammatory cytokines. This way we could determine how cytokines sensitize endothelial cell response with Aβ.

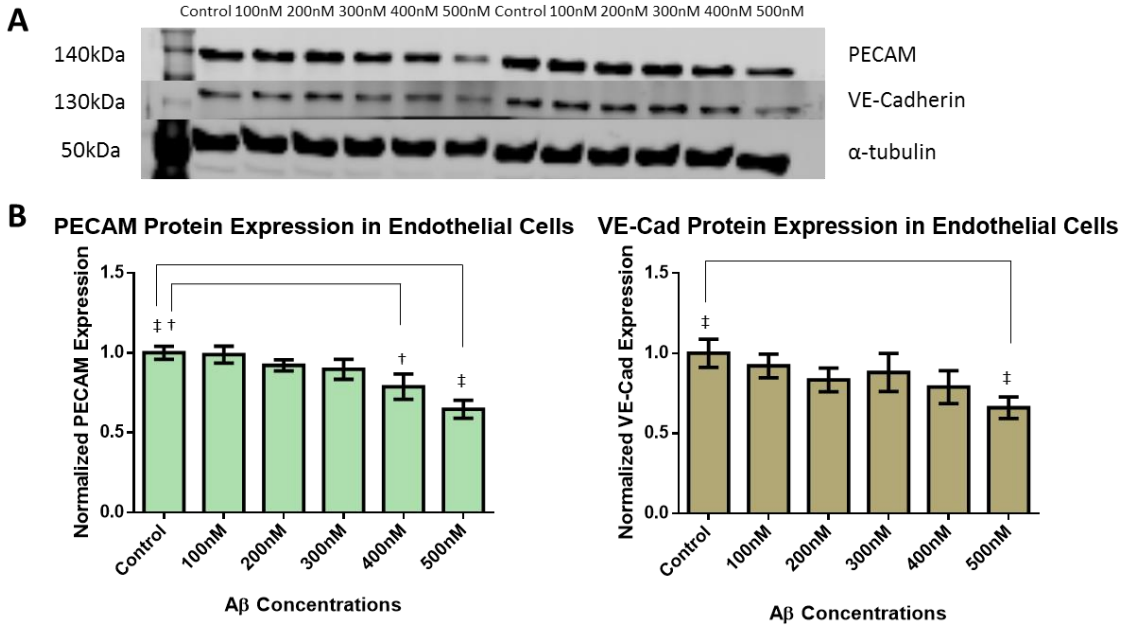

Figure 8 - Western blot analysis of hMVEC dose-response to Aβ. (A) Western blot showing PECAM, VE-Cadherin and α-tubulin expression of hMVEC 6-well plate cultures in control and Aβ concentrations ranging 100nM-500nM. (B) Fluorescent intensity values normalized to first α-tubulin intensity then controls. Significant reduction in protein expression were found in PECAM experiments at 400nM ($p = 0.026$) and 500nM ($p < 0.0001$) and in VE-Cadherin experiments at 500nM ($p = 0.0071$).

2.3 Preliminary Immunocytochemistry

Before engaging the study, we also wanted to characterize differences in junction protein expression in endothelial cells in response to upregulated cytokines in AD, VEGF and TNF-α, with and without Aβ. We also wanted to confirm our cell culture methods would work for this experimental setup and how using Matrigel would work in our system.

Therefore, the purpose of this experiment was to: 1) evaluate this platform's ability to grow endothelial cells against a protein scaffold to form a monolayer, 2) eliminate biochemical conditions for future studies based on cell loss and 3) identify Matrigel's efficacy for growing endothelial monolayers in our culture platform.

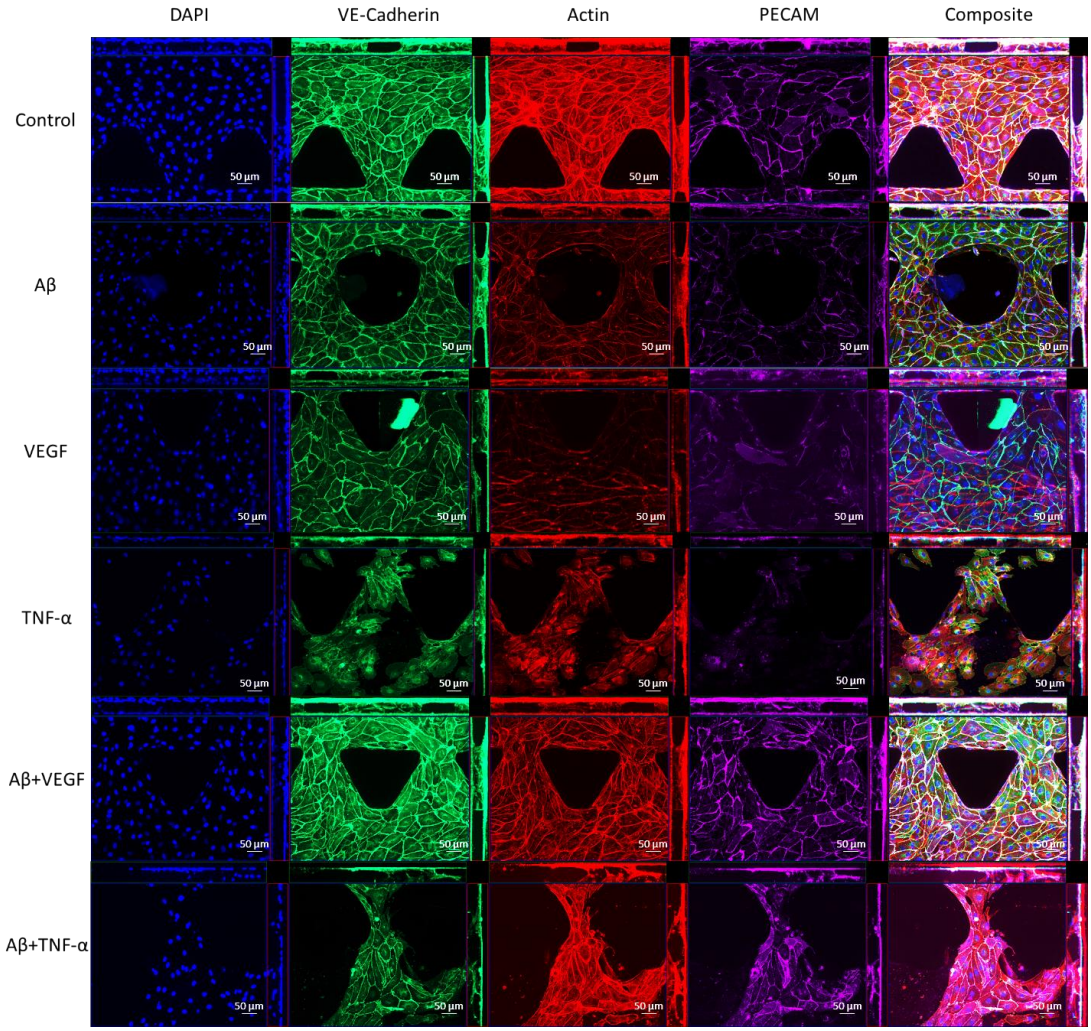

Figure 9 - Immunofluorescent staining for adheren junction proteins in hMVECs growing in 2.5mg/mL collagen and 3mg/mL Matrigel 1:1 mixture. Blue: Dapi. Red: Phalloidin. Green: VE-Cadherin. Purple: PECAM. Cells were grown for 7 days to ensure monolayer formation on all surfaces. Conditions were Control, 50nM Aβ, 50ng/mL VEGF, 20ng/mL TNF-α, 50nM Aβ + 50ng/mL VEGF and 50nM Aβ + 20ng/mL TNF-α and show respective junction protein expressions. Images are maximum intensity projections of the 3D microenvironment.

We conducted an immunofluorescent assay (Appendix A.4.2) with devices that had a collagen gel and Matrigel 1:1 mixture and endothelial cells that had grown for 5 days then conditioned for 24 hours. Immunofluorescent images, as seen in figure 9, reveal that TNF-α with and without Aβ leads to cell loss in endothelial cell cultures and therefore decreases the total PECAM and VE-Cadherin protein expression. From this data, we decided that TNF-α would be our positive control for our experimental setup and testing TNF-α with Aβ would be redundant for our experimental setup, despite the reports of upregulated secretion of TNF-α in human brains [5]. Subtle changes in protein fluorescence can be seen in Aβ and VEGF conditions, therefore analyzing with immunocytochemistry in these devices is difficult. Slight morphological changes are observed, however, a lack of discernible differences in PECAM or VE-Cadherin protein expression drove a change in our methodology, where we measure protein expression only on the scaffold wall. We speculate cell invasion into the gel is likely caused by growth factors within the Matrigel, leading to endothelial cells growing towards growth factors and degrading the gel. We decided that devices with so much invasion into the gel region could not be used for analyzing fluorescent intensity of PECAM and VE-Cadherin. Rather, future experiments required that we form a monolayer against the gel and channel threshold to isolate a region that could be consistently measured for junction protein expression. We also observed that Matrigel could not be used for these experiments because it caused inconsistent and extensive cell invasion. Though Matrigel is more physiologically relevant for the brain microenvironment [53, 55, 64], collagen better enables endothelial monolayers to form, providing an ideal scaffold with which to quantify barrier function through junction protein expression in 3D [20]. Therefore, we used a 2.5mg/mL collagen matrix for all the following

experiments because it consistently is more stiff and less prone to extensive cell invasion [65].

We also wanted to ensure that our microfluidic cell culturing device was functional for endothelial cell growth patterns as displayed in figure 10 [37, 58]. Since endothelial cells grow into monolayers on surfaces, we created a 3D rendering of a z-stack to examine the 3D growth patterns within our device design [58]. Endothelial cells in our microfluidic device cell culture platform grow to form monolayers on the glass slide, the polydimethylsiloxane (PDMS) surface at the top of the channel and the PDMS surface of the posts which can be seen in figure 10. Isometric and side views of the imaging area clearly show that endothelial cells grow in the desired monolayer fashion in our devices despite the cell invasion into the gel region. We therefore, demonstrate, with preliminary device cultures, that our microfluidic device allows for endothelial cells to form a monolayer to form a barrier along the z-direction, against which we can measure barrier function and transport across the monoalyer.

2.4 Dextran Diffusion in Aβ and Inflammatory Conditions

Diffusion experiments are extensively used to determine monolayer functionality in endothelial cells and epithelial cells [3, 66]. Experimentally, diffusion can be characterized in several different ways: functional MRI, Evan's blue dye and FITC dextran for *in vivo* experiments [13, 67, 68]; and FITC dextran and trans-endothelial electrical resistance (TEER) for *in vitro* experiments. Functional MRIs track blood flow in live brains with an injected radiolabel and can detect leakiness from blood vessels [13]. Evan's blue dye can be injected intravenously, which cannot diffuse through healthy brain vasculature,

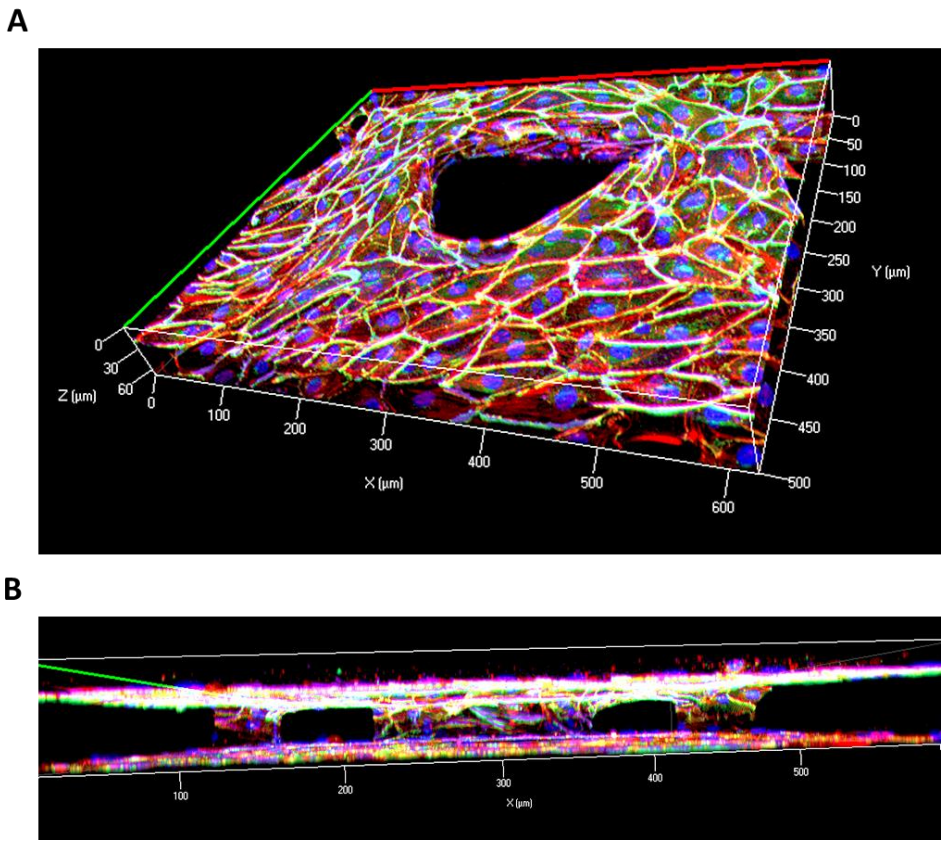

Figure 10 - Immunofluorescent images demonstrating a clear 3D growth pattern where hMVECs form a monolayer on the top, bottom and posts of the device. Blue: Dapi. Red: Phalloidin. Green: VE-Cadherin. Purple: PECAM. (A) Isometric view of 3D microenvironment within the device. (B) Side view demonstrating cells grow to form monolayers on top, bottom and on posts while leaving an opening in between the surfaces to generate vessel-like constructs.

however, can diffuse through disease brain vasculature [68]. Evan's blue is commonly used in animal models where animals are sacked and tissues are analyzed [68]. TEER is used to measure the electrical resistance across an endothelial monolayer, where higher electrical resistances indicate homeostatic barrier function in endothelial cell monolayers [54]. FITC dextran are fluorescent beads that come in various sizes and can diffuse through barriers based on the pore size [67]. Brain microvasculature has been shown to prevent 70kDa dextran diffusion in healthy brains, however, becomes leaky and allows 70kDa dextran

diffusion in brains affected by AD [51]. Therefore, we chose to use 70kDa dextran for characterizing the barrier function of our endothelial cell monolayers.

Our data, collected via protocols in Appendix A.3, are consistent with previous studies of endothelial monolayer permeability to 70kDa dextran, showing low diffusion in control samples. We normalized fluorescent intensity to controls and our data show a significant increase in endothelial cell monolayer permeability in all other conditions. This is expected, particularly in VEGF and TNF-α conditions, because of how these proteins modulate adheren junction protein expression. TNF-α is extensively characterized to cause apoptosis in most cell types [5, 69] and it has been demonstrated in our experimental setup to lead to cell loss in endothelial cell cultures, thus allowing dextran diffusion. Studies have also characterized downstream signaling of VEGF receptor 2 activation which includes downregulation of VE-Cadherin expression and therefore a decrease in cell-cell adhesion, contributing to our hypothesis that upregulation of pro-inflammatory cytokines such as VEGF leads to endothelial monolayer permeability. Subsequently, Aβ has also been shown to interact with growth factor receptors [70, 71], including VEGF receptor 2 [70], possibly contributing to endothelial monolayer permeability as shown in our transwell plate permeability studies shown in figure 11.

Though our transwell data demonstrates endothelial monolayer permeability to dextran in response to our testing conditions, the complexity of biochemical interactions warrants further characterization of diffusion through an endothelial monolayer in a more physiologic culture platform. We further characterized diffusion through an endothelial monolayer by culturing endothelial cells in our microfluidic device. We established an endothelial monolayer against the protein scaffold in our microfluidic platform and

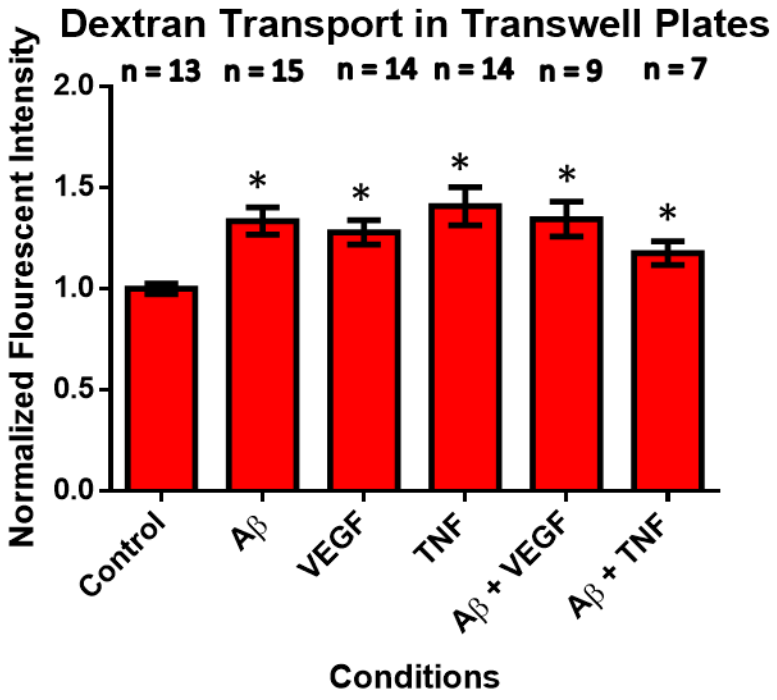

Figure 11 - Dextran Diffusion shows endothelial cell monolayer permeability in response to inflammatory cytokines and Aβ in transwell plates. Fluorescent intensity of diffused dextran in various conditions with background subtracted and normalized to controls. Bars represent standard error of the mean with a significant difference established between Control and every other condition ($p<0.05$) using one-way ANOVA and Brown-Forsythe post hoc tests.

conditioned our cells for 24 hours. Then, dextran was added to the channel with the monolayer and allowed to diffuse throughout the device for 18 hours. Transport across the monolayer is indicated by increased fluorescent intensity in the protein scaffold gel region. Fluorescent intensity of each imaging region was normalized to fluorescent intensity within the channel. These values were averaged to generate normalized fluorescence (F_N) as displayed in figure 12B. Our microfluidic culture platform shows similar trends to our transwell data, and better visualizes the nature of diffusion through an endothelial monolayer as can be seen in figure 12A. Diffusion was quantified using fluorescent

intensity of dextran past a threshold of the gel layer where figure 12 clearly displays how far across the gel the dextran can diffuse.

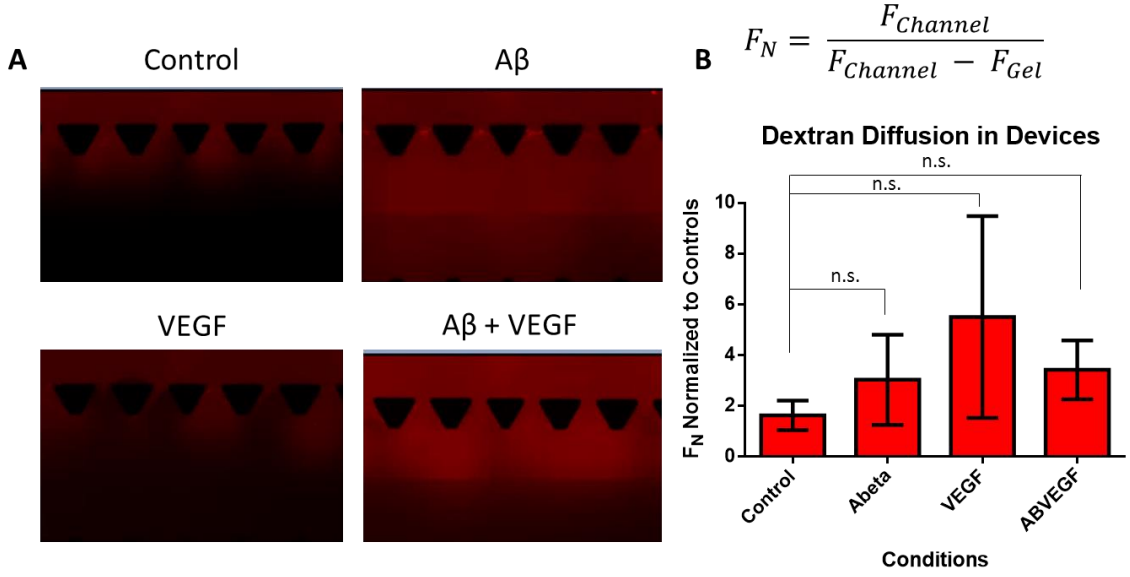

Figure 12 - Dextran Diffusion shows endothelial cell monolayer permeability in both transwell plates and microfluidic devices. (A) Fluorescent images of diffused dextran in various conditions. (B) Fluorescent intensity quantification showing diffusion through endothelial cell monolayer into the collagen gel region in microfluidic devices. Bars represent standard error of the mean and no statistical significance was established (n = 4).

OUTCOME: This integrated characterization of dextran diffusion shows clear functional changes in endothelial monolayer permeability in transwell plates, however, our microfluidic quantification method is still ongoing. To better understand these results, we decided to further investigate changes in endothelial cell function by quantifying junction protein expression and angiogenic growth.

2.5 Quantification of Barrier Function

After looking at dextran transport, a method for measuring barrier function in endothelial cells, we wanted to quantify protein expression of both PECAM and VE-Cad, two major adheren junction proteins ubiquitously expressed in endothelial cells [32, 33, 41, 57]. An integrated approach utilizing both traditional 2D well plate cultures for western blot analysis and innovative 3D microfluidic cultures to quantify differences in PECAM and VE-Cad protein expression across conditions.

Western blot quantification of adheren junction protein expression (Appendix A.4.1) shows inflammatory cytokine and Aβ stimulated conditions decrease PECAM and VE-Cad protein expression which can be seen in figure 13. Significant differences were observed from control to Aβ ($p=0.029$), TNF-α ($p<0.0001$), and Aβ + TNF-α ($p<0.0001$) in PECAM protein expression; and control to TNF-α ($p=0.0025$) and Aβ + TNF-α ($p=0.013$) in VE-Cad protein expression. A significant difference was also observed from VEGF to Aβ + VEGF in VE-Cad protein expression ($p=0.015$). This outcome is likely due to known influences of TNF-α and VEGF on decreasing endothelial cell junction protein expression [72, 73]. Also, as previously stated, Aβ has been shown to interact with growth factor receptors. Therefore, decreases in protein expression for Aβ conditions as shown in figure 13 are comprehensible as well [42]. This method utilizes 6-well plate culture methods which are commonly used for western blot analysis for protein expression [42]. This method also allows endothelial cells to form a monolayer and develop cell-cell adhesion. However, cells are growing on polystyrene with this method which is not as physiologic as a protein scaffold [19, 64]. Therefore, we decided to quantify barrier function using our microfluidic culture platform where endothelial cells grow against a

collagen scaffold in 3D to form a monolayer, establishing a more physiologic microenvironment [19, 64].

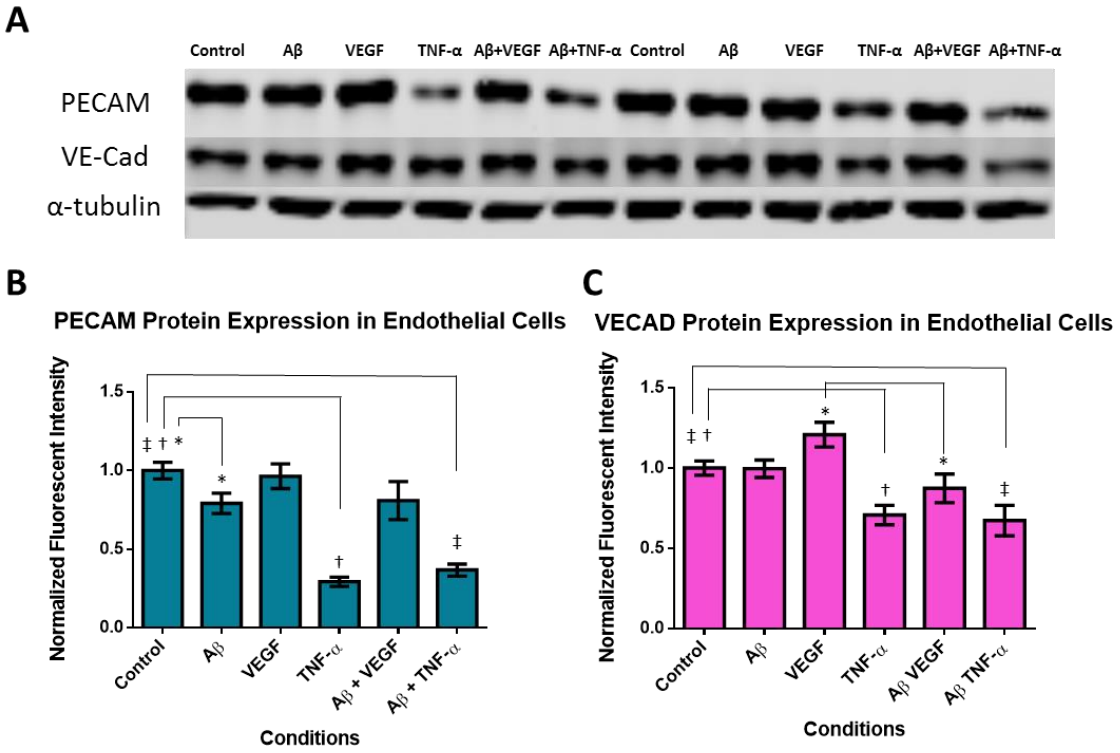

Figure 13 - Western blot analysis shows endothelial cell monolayer protein expression in 6-well plate cultures. (A) Membranes, fluorescently imaged with Li-Cor imaging system, show protein expression with respect to conditions and loading controls. (B) Quantification of PECAM protein expression in response to the various conditions: Vehicle, 300nM Aβ, 50ng/mL VEGF, 20ng/mL TNF-α, 300nM Aβ+50ng/mL VEGF and 300nM Aβ+20ng/mL TNF-α shows a trend where all conditions downregulate protein expression, however, no statistical significance was established. (C) Quantification of VE-Cad protein expression shows similar trend to PECAM also with no statistical significance established (n = 4 for all).

Microfluidic device cultures were grown until an endothelial monolayer formed and later fluorescently stained for PECAM and VE-Cad (Appendix A.4.2). Representative images of conditions are in figure 14A, and show subtle differences in protein expression that cannot be qualitatively analyzed, therefore, we decided to quantify the fluorescent

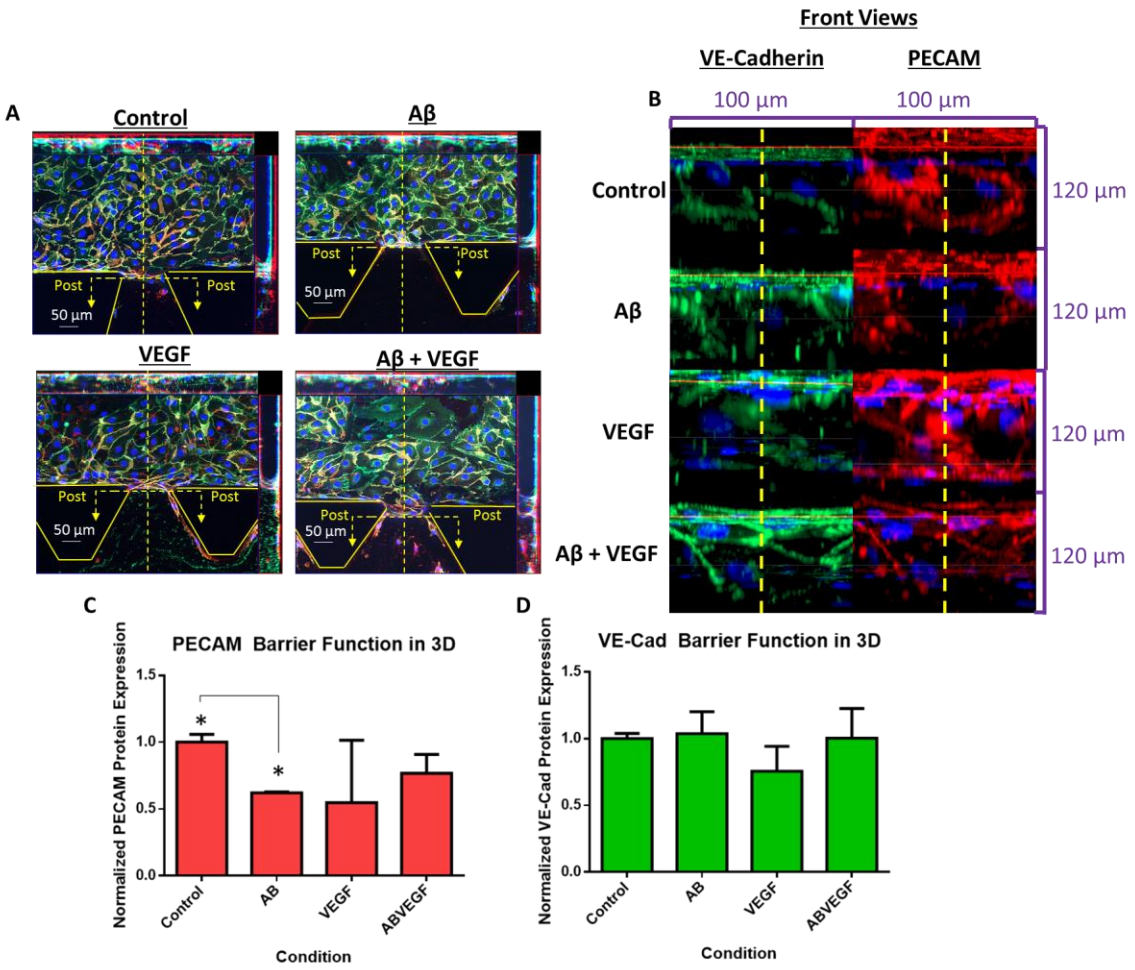

Figure 14 - Quantification of barrier function using fluorescent intensity of a 3D monolayer grown against the collagen scaffold. (A) Representative images showing monolayer against the protein scaffold quantified for each condition. Images are maximum intensity projections of the 3D microenvironment. (B) Images depict sections demonstrating front views of 3D rendered devices from images in part A. (C) Quantification of barrier proteins were normalized to cell count and demonstrates statistically significant downregulated PECAM expression in response to Aβ (p = 0.007), but not other conditions (n = 3). (D) VE-Cad quantification shows no significant changes in protein expression or a trend (n = 3).

intensity of the monolayer/gel threshold region of each device's maximum intensity projection image. We normalized fluorescent intensity to the number of cells contributing to the monolayer which was counted via DAPI staining. Quantification of PECAM and VE-Cad along the protein scaffold show significant decreases in protein expression in only

the Aβ condition in PECAM as shown in figures 14B and 14C. Other conditions did not establish statistical significance, however, a trend demonstrating the influence of VEGF and Aβ can be seen in the PECAM quantification.

Our data show barrier protein expression, an important aspect of characterizing changes in endothelial cell function, is decreased in Aβ and inflammatory cytokine conditions. However, statistical significance could not be established in most cases, most likely due to the low sample size of both experiments. Nevertheless, this integrated approach of 2D and 3D cultures is advantageous for fully characterizing barrier function in endothelial cell monolayers due to the benefits of both simplicity in well plate cultures and microfluidic device physiologic relevance.

2.6 Reduced Angiogenic Growth in Aβ Conditions

Angiogenesis is another major function of endothelial cells and, as previously mentioned, has been shown to be downregulated in AD tissues [70, 74]. Therefore, we decided to interrogate changes in angiogenesis in response to VEGF and Aβ with protocols detailed in Appendix A.5. Cells were grown for 24-48 hours in devices to avoid cell invasion into the gel prior to preparation and conditioning for the angiogenesis assay, which can be referenced in figure 25, located in the Appendix. Quantification strategy can be seen in figure 15, where we measured the distance travelled by angiogenic sprouts after 48 hours of conditioning in each region between two posts in every device. These distances were measured via matlab, where we selected two points on each image for starting and finishing positions for branches and calculated the distance travelled with a simple distance between two points equation as shown below (D_B stands for distance of the branch).

$$D_B = \sqrt{(x_1 - x_0)^2 + (y_1 - y_0)^2} \quad (1)$$

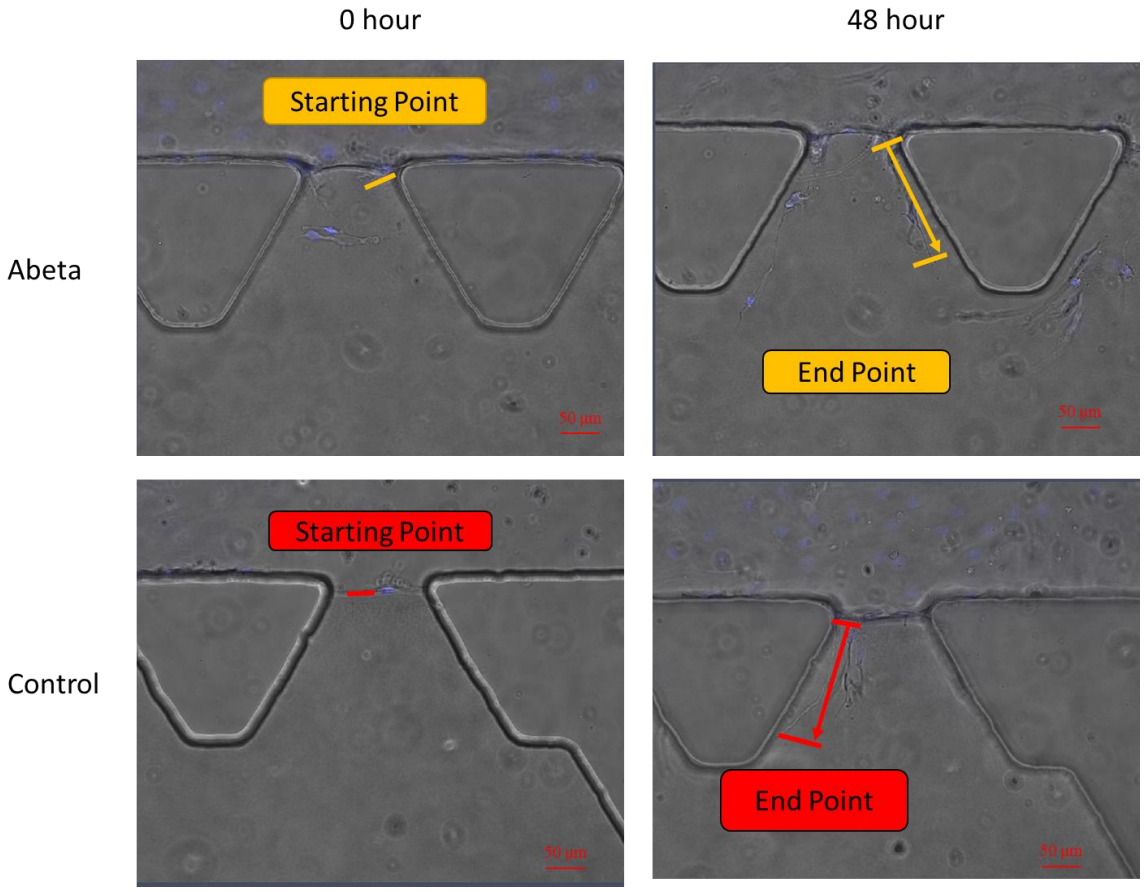

Figure 15 - Phase contrast and live cell fluorescent imaging for tracking angiogenic sprouting of hMVECs grown in 2.5 mg/ml collagen gel at 0 and 48 hours for Control and VEGF stimulated conditions. Graphics demonstrate the method used to quantify the distances of angiogenic sprouting.

Quantification of angiogenic growth demonstrates that Aβ decreases angiogenic sprouting with respect to control and VEGF conditions which can be seen in figure 16. We expected VEGF to have higher angiogenic growth than our control, but did not see that in our analysis. In fact, Previous studies have shown that this method of stimulation and VEGF gradients should increase angiogenic sprouting distances [46], but we did not observe that trend. Moreover, statistical significance was established between: control and

Aβ, VEGF and Aβ+VEGF, and Control and Aβ+VEGF, demonstrating a functional change in angiogenic growth of endothelial cells in response to Aβ. These data suggest that our microfluidic cell culture platform and method for quantifying angiogenic growth can model changes in angiogenesis with respect to inflammatory cytokines upregulated in AD and Aβ.

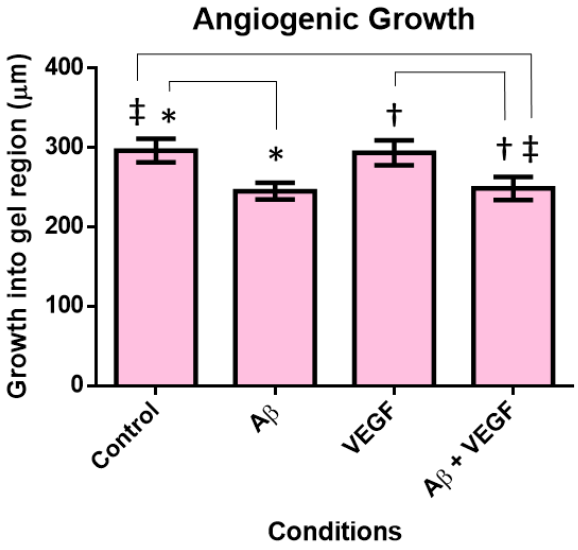

Figure 16 - Quantification of angiogenic growth, as measured with the technique shown in figure 15, demonstrates Aβ decreases angiogenic sprouting distances into the gel region with respect to both Control and VEGF conditions. Statistical significance was established between control and Aβ (p = 0.005), VEGF and Aβ+VEGF (p = 0.037), and control and Aβ+VEGF (p = 0.023) with (n = 105 growth regions from 3 devices) using one-way ANOVA and post hoc tests.

Combined, endothelial monolayer permeability, junction protein expression and angiogenic growth are strong metrics for characterizing endothelial cell response to inflammatory cytokines in AD and Aβ [20, 46, 73]. However, we can further characterize changes in endothelial cell function by looking at intracellular signaling, since intracellular signaling drives several processes in cellular function [75]. We therefore concluded that

intracellular signaling is a key component for identifying a core signaling pathway that is driving functional changes in endothelial cells, or, in the context of AD, pathogenesis.

2.7 Upregulated MAPK Signaling in Aβ and Pro-Inflammatory Conditions

Recent human Alzheimer's post-mortem tissue studies have demonstrated upregulated p38 and ERK MAPK signaling [76]. MAPK signaling has several pathways, of which ERK has been linked to upregulation of angiogenesis in endothelial cells [48, 72, 77]. However, as mentioned earlier, AD tissues have also shown a lack of angiogenic growth establishing that despite an increase in angiogenic signaling there is little new development of brain vasculature in AD [28, 74]. This suggests that p38 MAPK intracellular signaling changes in endothelial cells could be driving pathogenesis of AD, which in the context of VEGF and TNF-α receptor activation along with downstream effects, can be seen in figure 17. Therefore, we elected to conduct a MAPK intracellular signaling analysis.

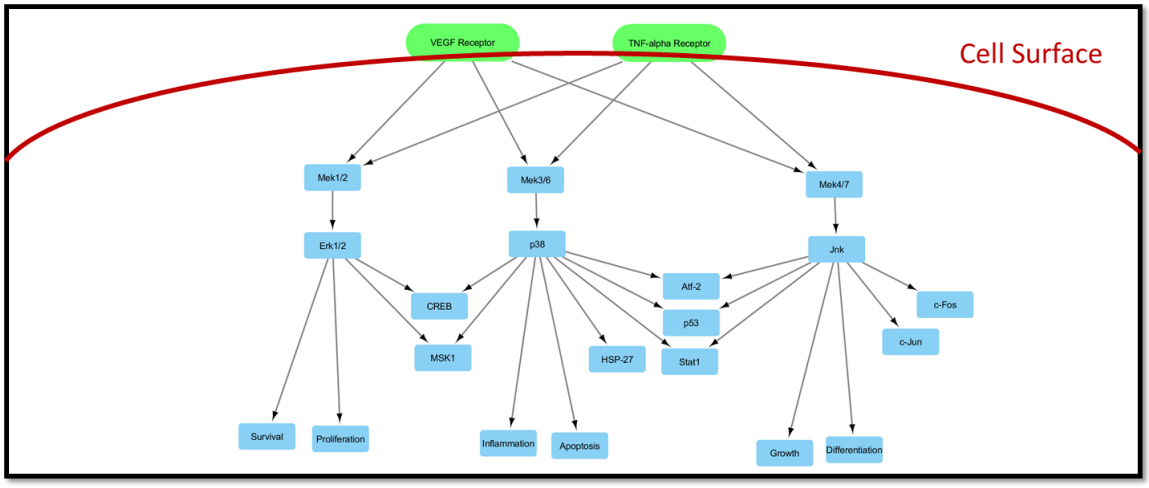

Figure 17 – MAPK intracellular signaling pathway in the context of VEGF and TNF-α receptor activation.

For this experiment, we collected cell lysates from endothelial cell cultures from both a traditional 6-well plate method and our microfluidic platform (more detailed methods are described in the Appendix A.6). We then followed the protocol for a Luminex multiplex MAPK bead-based immunoassay to quantify changes in phospho-proteins in the MAPK signaling pathway. Readouts were fluorescent intensity values associated with overall expression of each analyte. Data was processed using MATLAB to complete a partial least squares regression (PLSR) statistical analysis. In general, PLSR is a method for creating new axes called latent variables (LV) where the X variables (analytes) are weighted based on the measurements of each analyte. PLSR is particularly useful here because we have a small sample size and more analytes than readouts per condition [78, 79] and PLSR can account for the X variables that are linearly related to each other. Using PLSR, we were able to identify top correlates of analytes with respect to each sample [79], determining which analytes are most correlated with our conditions. Figure 18 demonstrates that in part B (partial least squares discriminant analysis, PLSDA), control samples are most correlated with the negative spectrum of LV1 which is organized in part C, and shows pc-Jun, pStat1 and p-p53 phospho-proteins are most correlated to control samples. Therefore, we can identify that control samples are most correlated with the c-Jun MAPK signaling pathway with respect to our other conditions. Conversely, Aβ, VEGF and Aβ+VEGF conditions show increases in pHSP-27, pErk1/2 and p-p38. We can then deduce that Erk and p38 MAPK signaling pathways are both upregulated, however, p38 is more upregulated due to HSP27 being downstream of p38 [80, 81]. Additionally, our data shows Aβ+VEGF samples have further p38 MAPK signaling upregulation due to a high correlation to the negative spectrum of LV2. As mentioned earlier, post-mortem AD tissue

studies have shown upregulated p38 MAPK signaling [76]. Therefore, these results match previous studies, likely because we conditioned endothelial cells with Aβ and the top cytokine correlate, VEGF [5], generating a micro-environment slightly mimicking AD.

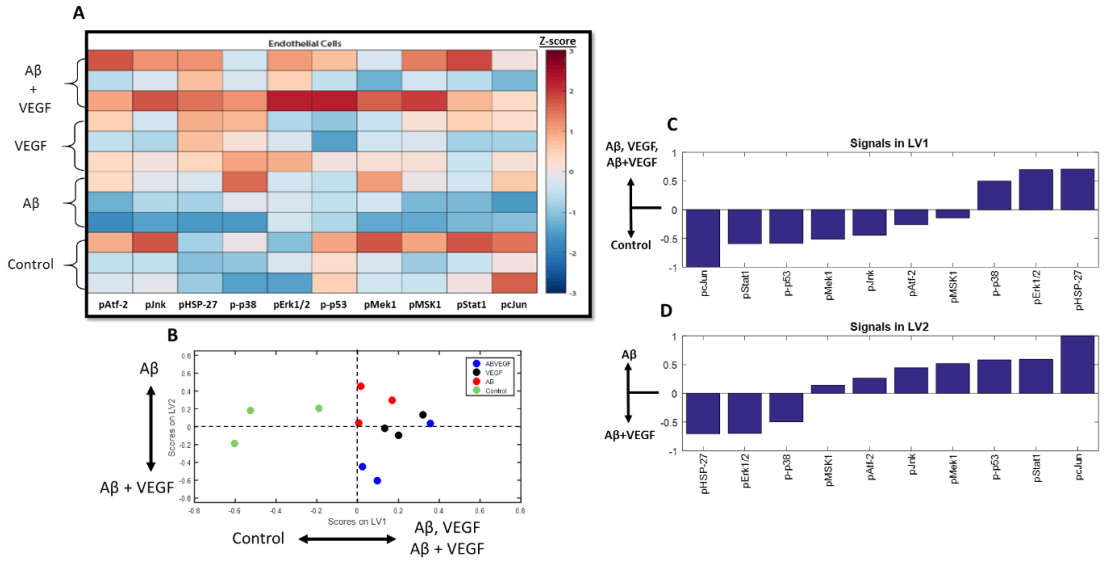

Figure 18 - Partial least squares regression of intracellular signaling MAPK readings. (A) Heatmap shows intensity of phosphorylated MAPK protein expression in harvested cells lysates in 4 conditions: Control, 50nM Aβ, 50ng/mL VEGF and 50nM Aβ + 50ng/mL VEGF. (B) Partial least squares discriminate analysis of the 4 conditions shows separation of conditions along latent variables (LVs) 1 and 2. (C-D) Latent variables were calculated and show protein expression that are upregulated or downregulated with respect to z-score of conditions along each latent variable as shown in part (B).

We also completed our PLSR statistical analysis including readouts from our positive control, TNF-α. Overall, TNF-α samples had such a strong intracellular signaling response that analyzing signaling correlations in other conditions was difficult. Because PLSR determines latent variables from the entire data set, the strong signals in TNF-α samples caused a major shift in the PLSDA. This led to the generation of latent variables that were heavily influenced by signals that were upregulated in TNF-α conditions.

Consequently, this caused signals from other conditions to be aligned differently within our latent variables, showing little separation from samples other than TNF-α. In short, excluding TNF-α from our PLSR analysis completely changed the correlation of analytes to conditions and provided a true analysis in signaling differences with respect to the subtle changes observed in endothelial cells in response to Aβ and VEGF.

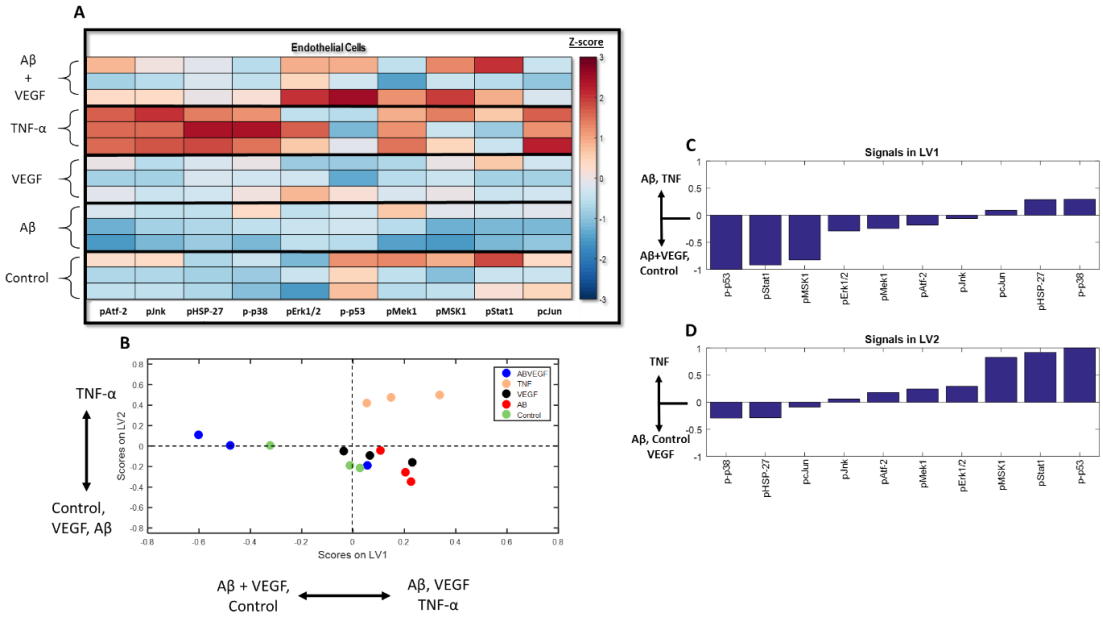

Figure 19 - Partial least squares regression of intracellular signaling MAPK readings. (A) Heatmap shows intensity of phosphorylated MAPK protein expression in harvested cells lysates in 4 conditions: Control, 50nM Aβ, 50ng/mL VEGF and 50nM Aβ + 50ng/mL VEGF. (B) Partial least squares discriminate analysis of the 4 conditions shows separation of conditions along latent variables. (C-D) Latent variables were calculated and show protein expression that are upregulated or downregulated with respect to z-score of conditions along each latent variable as shown in part (B).

Interested in determining signaling differences with respect to 3D versus 2D culture methods, we then decided to extend our PLSR analysis to samples collected from our microfluidic culture platform. We expected to see differences due to enhanced physiologic

culture conditions. Our 3D data, displayed in figure 20, show similar trends where VEGF and Aβ+VEGF conditions were highly correlated with p38 MAPK signaling, showing

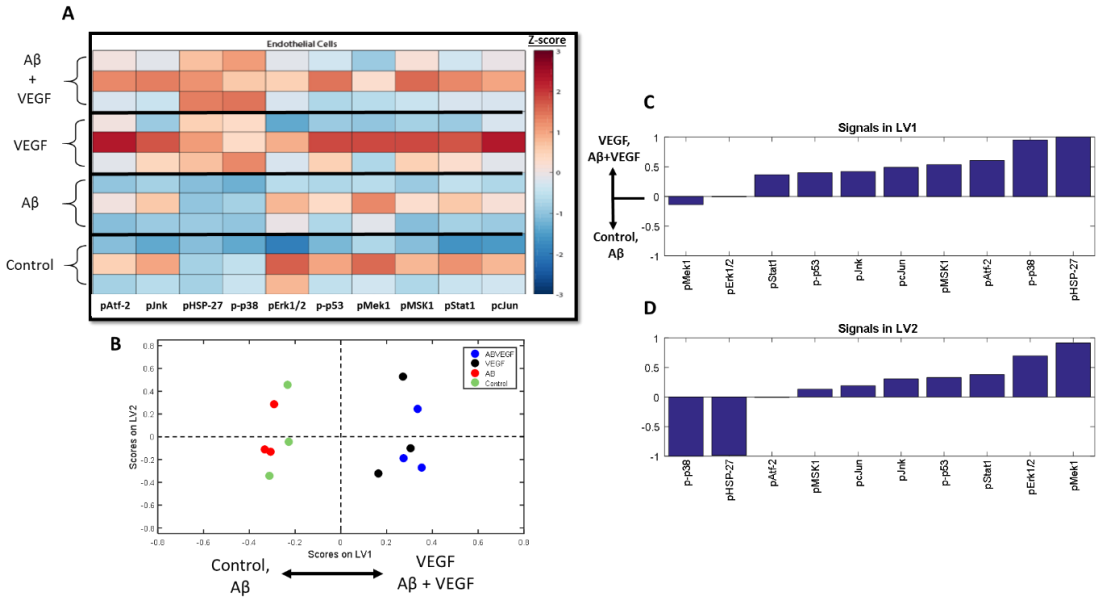

Figure 20 - Partial least squares regression of intracellular signaling MAPK readings. (A) Heatmap shows intensity of phosphorylated MAPK protein expression in harvested cells lysates in 4 conditions: Control, 50nM Aβ, 50ng/mL VEGF and 50nM Aβ + 50ng/mL VEGF. (B) Partial least squares discriminate analysis of the 4 conditions shows separation of conditions along latent variables. (C-D) Latent variables were calculated and show protein expression that are upregulated or downregulated with respect to z-score of conditions along each latent variable as shown in part (B).

heightened phosphorylation of HSP27 and p38. However, Aβ alone did not show a difference in MAPK signaling from control samples, unlike the 2D signaling analysis. This was not expected because we quantified differences in endothelial permeability, junction protein expression and angiogenesis in response to Aβ, all of which indicate stressed intracellular signaling within our microfluidic culture platform. This deviation could be attributed to several different factors two of which could be: 1) the protein scaffold could be causing cells to exhibit reduced inflammatory response due to changes in adhesion or

2) most of the cells were growing on either PDMS or glass which is different from the polystyrene in 2D experiments. Because there are several possible influences responsible for the drop in p38 MAPK signaling in response to Aβ in our 3D microfluidic culture platform, we conclude further study and validation is required.

CHAPTER 3. CONCLUSION

3.1 Contributions of This Work

This thesis has developed an integrated methodology utilizing both traditional and 3D cell culture platforms to characterize endothelial cell function in response to pathologically up-regulated proteins:

- I began by determining a dose of Aβ that would downregulate endothelial cell junction protein expression and possibly in turn monolayer permeability.
- I conducted dextran diffusion assays to quantify changes in endothelial monolayer permeability in response to Aβ and inflammatory cytokines. We discovered that Aβ, VEGF and TNF-α all increase endothelial monolayer permeability in both transwell culture methods.
- I demonstrated downregulation of barrier function in response to Aβ, VEGF, and TNF-α in 2D cultures and Aβ in 3D endothelial monolayers in our devices utilizing western blot and immunocytochemistry analytical tools.
- I determined angiogenesis is significantly downregulated in response to Aβ utilizing our 3D microfluidic culture platform.
- I characterized changes in intracellular MAPK signaling in both traditional 2D culture and innovative 3D microfluidic culture platforms. Endothelial cell stimulation by Aβ and VEGF, showed upregulation of p38 MAPK signaling. Signaling differences in 2D versus 3D culture methods were observed, however, several similarities indicates that our 3D microfluidic culture platform is capable of conserving endothelial cell signaling.

Combined, these results: 1) increased permeability through an endothelial monolayer, 2) downregulated junction protein expression, 3) decreased angiogenic sprouting, and 4) upregulated p38 MAPK signaling in response to Aβ, VEGF and TNF-α demonstrate an integrated method utilizing both traditional and more innovative culture methods. This thesis provides a complete framework by which changes in endothelial cell function are extensively characterized. This integrated approach will be useful for identifying upregulated signaling pathways that correspond to changes in endothelial cell function such as monolayer permeability or angiogenesis [48]. The identified pathways can then be targeted for inhibition to restore endothelial cell homeostatic function.

3.2 Future Directions

Based on our data, we have identified that the p38 MAPK signaling pathway is upregulated in response to VEGF and Aβ. Future directions include inhibiting p38 to determine if p38 restores homeostatic endothelial cell signaling and function [75, 76]. This would effectively identify a therapeutic strategy for restoring endothelial monolayer homeostasis in the context of vascular dysfunction in AD.

Based on our findings and development of the 3D microfluidic culture platform, more complex multi-cellular models of vascular dysfunction can be established utilizing our microfluidic culture platform. One currently popular area of research is in designing microfluidic devices that accurately model the BBB [19, 56]. Many microfluidic "brain on a chip" platforms have already been developed, each with various levels of complexity and physiologic relevance [19, 56]. Each are beneficial, however, not all can be adapted for characterizing endothelial monolayer permeability or angiogenesis [19]. The culture

platform used in this thesis can be further developed to include other cells found in the BBB, increasing physiologic relevance [19, 56].

Parallel to BBB models, improving our platform to construct a more physiologic microenvironment for vascular dysfunction in response to immune cell interaction is important for characterizing the effects of inflammation on endothelial monolayer integrity [82]. Inflammation is a popular research area, an area for which our microfluidic culture platform could easily be adapted. Much research in this area is focused on macrophage recruitment and activity [83, 84], and how they interact with the inflamed microenvironment [83, 84]. Since our device allows biochemical interactions between cells across the gel region, macrophages and endothelial cells could be simultaneously cultured in our device. Endothelial cell function can then be quantified in response to stimulated macrophages [84-86].

APPENDIX A. MATERIALS AND METHODS

A.1 Device Fabrication

Devices were fabricated out of polydimethylsiloxane (PDMS- Dow Corning Sylgard 184 mixed in a 10:1 ratio of elastomer base to crosslinking agent) by pouring into a plate containing a silicon wafer, created from common soft lithography techniques (ref [87]). Devices were cut out of the plate and holes were punched to form the reservoirs and filling ports. Devices were then suspended in DI water and autoclaved for 40 minutes on a liquid setting. Devices were then placed in 150mm diameter plates with feature sides faced up and placed in the oven overnight at 80℃ to dry. Devices were then plasma bonded to #1.5 glass cover slips (VWR – 48393-241) and placed back in the oven overnight at 80℃. Next, 1 mg/mL Poly-D-lysine (PDL) (Sigma-Aldrich) was pipetted throughout the entire device then placed in the incubator for 4 hours to enhance cell and collagen gel matrix adhesion. Afterwards, devices were rinsed 3 times with sterile culture water and placed back in the oven at 80℃ for 24-48 hours to dry and increase hydrophobicity.

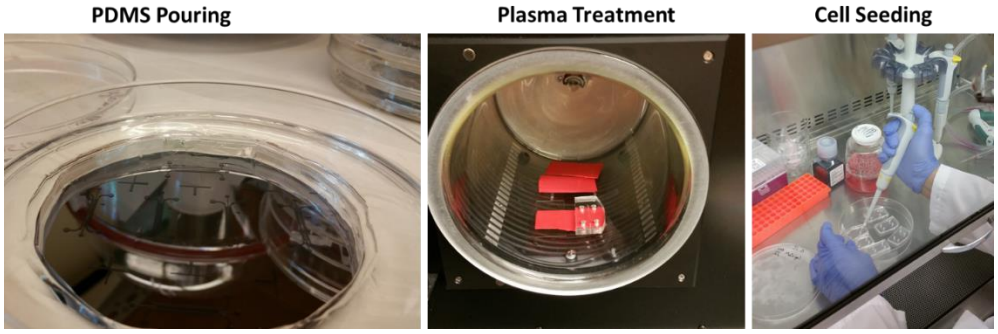

Figure 21 - Setup of various steps within device fabrication. Devices remain in a pseudo-sterile environment after autoclaving and maintain sterility during PDL treatment and cell culturing.

Collagen gel matrix was mixed together using type I collagen (Dow Corning - 354236), phenol red as a pH reader, NaOH and sterile culture water. 2.5 mg/mL collagen gel mixture at a pH of 8 was slowly pipetted into the gel ports to fill the gel region of each device to avoid spillage into channels. After collagen filling, devices were placed into humidified chambers inside the incubator for 2 hours to allow the collagen to polymerize. Channels on either side of the devices were filled with microvascular endothelial cell basal medium (Lonza EBM-2 Cat No. CC-3156) to hydrate the collagen matrix and prepare the device for cell culture.

A.2 Cell Culture

A.2.1 Passaging

Human microvascular endothelial cells (hMVECs Lonza – Cat No. CC-2543) were received at passage 3 and expanded to passage 6 in endothelial growth medium (Lonza EGM-2MV Cat No. CC-3202) via common cell culture methods. At passage 6 cells were cryogenically frozen until needed. When cells were needed for cell culture, a passage 6 vial was thawed and expanded. Cells for culture were used from passages 7-9 which maintained proliferation and endothelial function up to passage 10.

Upon cells reaching 70-90% confluency, cells were trypsinized (Sigma-Aldrich Trypsin-EDTA Solution Cat No. T3924-100ML), centrifuged and resuspended in endothelial growth medium to a density of 2.5 million cells/mL.

Time lapse angiogenesis experiments used live cell stain CellTracker Green CMFDA (Thermo Fisher Scientific Cat. No. C2925) at 1μg/mL and Hoechst 33342

(Thermo Fisher Cat. No. H3570) at 100ng/mL in the flask before cell seeding. These stain concentrations had no noticeable effect on cell survivability during culturing in devices.

A.2.2 Seeding Cells into Devices

To prepare the device for cell seeding, volumes specified below were pipetted into channel reservoirs to form a pressure gradient against the gel region on the cell side. This led to a small amount of flow across the gel region to ensure cell growth along the protein matrix. Devices were placed in the incubator and cells were allowed to flow through the channel until flow reached equilibrium and cells adhered to the protein matrix (about 2 hours). Endothelial growth medium was then added to top off the reservoirs to avoid cell death and devices were placed in the incubator overnight.

Medium in devices was replaced every 24 hours for the duration of their use. Cells were allowed to grow for various amounts of time: 24-48 hours for angiogenesis experiments, 72 hours for dextran and immunofluorescence experiments and 72+ hours for intracellular signaling experiments. Progressive lumen development and angiogenic invasion could be seen in longer growth periods, thus why angiogenesis and dextran experiments were completed with a lower growth period after cell seeding. Devices were then conditioned with: vehicle, Aβ, VEGF or Aβ+VEGF after the respective growth period for each experiment.

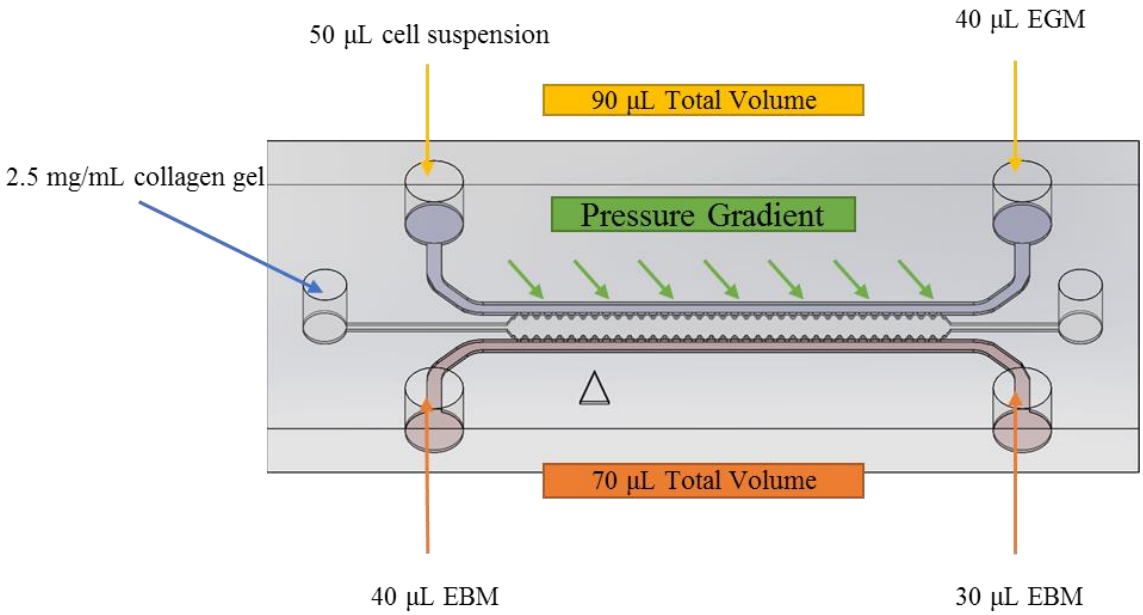

Figure 22 – Demonstration of the technique for cell seeding into devices

A.3 Dextran Permeability

Dextran experiments were conducted after a 72 hour growth period, when sufficient cell growth forms a cell monolayer against the collagen scaffold. Condition was induced and left to incubate for 4 hours to establish flow and pressure equilibrium. 1 µL of concentrated 5 mg/mL dextran was then added to one reservoir on the cell side and 1 µL of EBM was added to the opposite channel to maintain an equal pressure gradient. After the addition of dextran, devices were allowed to incubate overnight. Fluorescent images were taken at 18 hours with our fluorescent microscope (Zeiss Microscopy) across the entire device. Images were processed with Matlab (Mathworks) to determine fluorescent intensity of the gel region versus the cells channel. Normalized fluorescent intensity was calculated with the following equation:

$$F_N = \frac{F_{Channel} - F_{Gel}}{F_{Channel}} \quad (2)$$

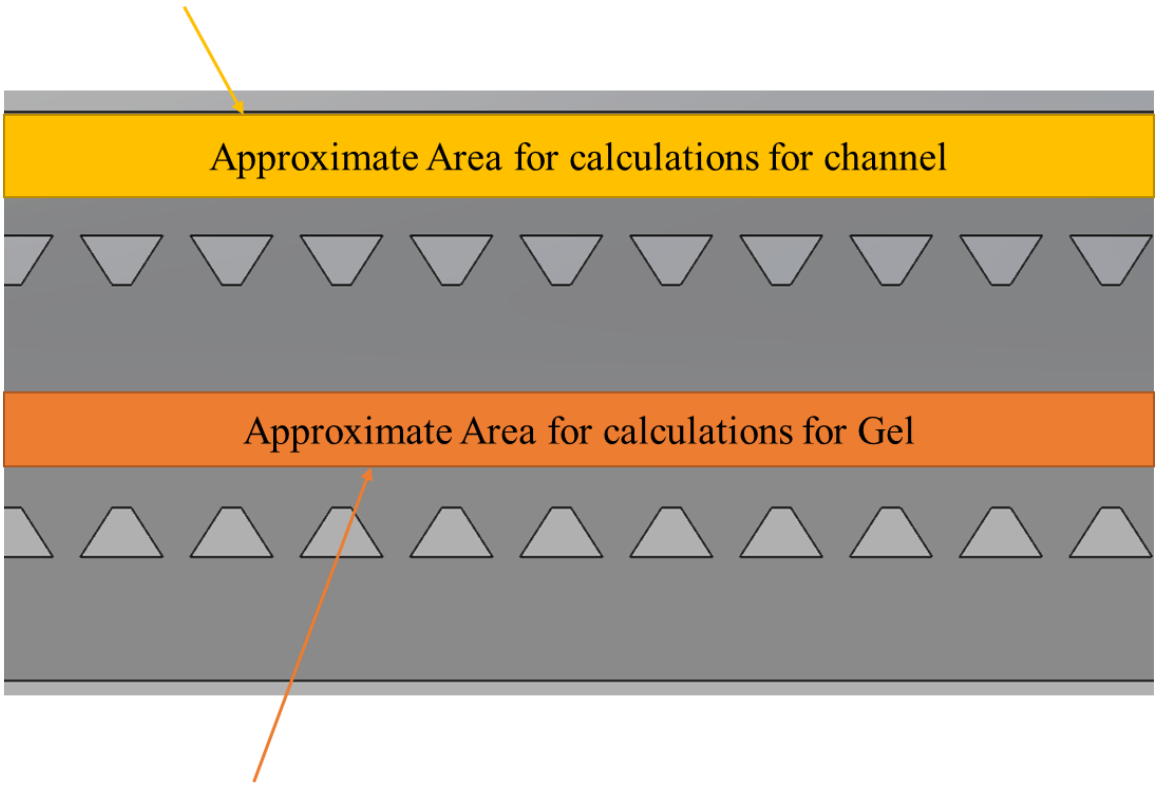

Figure 23 - Approximate regions for fluorescent intensity readings for dextran diffusion.

A.4 Junction Protein Quantification

A.4.1 Western Blots

Cells were seeded at $1x10^5$ cells/well in 6-well plates and grown to 90% confluence. Cells were then conditioned with: Vehicle, Aβ, VEGF, TNF-α, Aβ+VEGF or Aβ+ TNF-α for 24 hours. Cell lysis buffer was mixed using RIPA buffer (Boston BioProducts – Cat No. BP-115) with complete mini protease inhibitor tablets (Sigma Aldrich – Cat No. 11836153001), phosphatase inhibitor cocktail 2 (Sigma Aldrich – Cat No. P5726-5ML) and phosphatase inhibitor cocktail 3 (Sigma Aldrich – Cat No. P0044-5ML). Plates were transferred from the incubator onto ice, aspirated for the medium and rinsed with cold 1x

PBS (Corning – Cat No. 21040CM) once. Wells were aspirated and 140 µL of cell lysis buffer was added to the top of each well. Cells were then detached with a cell scraper and pipetted to micro-centrifuge tubes and placed on an inverter at 4℃ for 10 minutes. Lysates were then centrifuged at 4℃ and carefully pipetted into different tubes to discard cell debris. Lastly, lysates were stored in a -80℃ freezer.

Common western blotting buffers such as 10X tris buffered saline with Tween® 20 (TBST), running buffer and transfer were pre-made before conducting a western blot experiment. The following table details how these reagents were mixed.

Table 1 - Mixing ratios for creating common western blotting buffers. Reagents for creating buffers include trizma base (Sigma Aldrich – Cat No. T1503-5KG), glycine (Alpha Aesar – Cat No. J64365-A1), 20% SDS (Sigma Aldrich – Cat No. 05030-500ML-F) and NaCl (Aldon Corp SE – Cat No. SS0450-500G).

Transfer Buffer (10x) – pH 8.5

Tris	**30.3 g**
Glycine	142.5 g
DI Water	990 mL

Running Buffer (10x) – pH 7.4

Tris	**30.3 g**
Glycine	142.5 g
20% SDS	10 mL
DI Water	990 mL

TBST (10x) – pH 7.4

Tris	**12.1 g**
NaCl	87.6 g
Tween 20	500 uL
DI Water	990 mL

Blots were performed with homemade gels. 8 µg of each lysate was mixed with 4x Laemmli sample buffer (Bio-Rad – Cat No. 1610747) mixed 9:1 with β-Mercaptoethanol (BME, Sigma Aldrich – Cat No. M6250-100ML) and boiled for 5 minutes. Samples were then pipetted into lanes on the gel and left to run for 150 minutes at 80 volts. After running gels were rinsed in transfer buffer and protein was then transferred to PVDF membanes (GE Healthcare – Cat No. 10600023) for 75 minutes at 100 volts. Membranes were then blocked for 1 hour using Li-Cor blocking buffer (LI-COR Biosciences – Cat No. 927-

50003) and incubated in PECAM primary antibody from mouse (Cell Signaling Technologies – Cat No. 3528S), VE-Cadherin primary antibody from Rabbit (Cell Signaling Technologies – Cat No. 2500S) and α-tubulin primary antibody from mouse (Sigma-Aldrich – Cat No. T6074-200UL) suspended in Li-Cor blocking buffer overnight at 4℃. Membranes were then washed with 1x TBST and incubated in Alexa Fluor 680 anti-mouse (Thermo Fisher Scientific– Cat No. A-21058) and Alexa Fluor 790 anti-Rabbit (Thermo Fisher Scientific – Cat No. A11369) secondary antibodies for 1 hour at room temperature on a rocker. Membranes were then washed again with 1x TBST and imaged. Fluorescent intensity was measured within Image Studio software (LI-COR Biosciences) and processed with Matlab.

A.4.2 3D Barrier Immunofluorescence

Devices were given 72 hours for cells to grow and form a complete monolayer against the collagen gel matrix. Cells in devices were then conditioned with: Vehicle, 300nM Aβ, 50ng/mL VEGF or 300nM Aβ + 50ng/mL VEGF and left in the incubator for 24 hours. Afterwards, devices were rinsed with 1X PBS and crosslinked by flowing 4% paraformaldehyde (Electron Microscopy Sciences – Cat No. 15700) through the channels for 15 minutes. Devices were then rinsed with 1X PBS twice and solubilized with 0.1% Triton X (Sigma Aldrich – Cat No. X100-100ML) for 10 minutes. Devices were rinsed once with 1X PBS and blocked for 1 hour with blocking buffer: 5% BSA (VWR – Cat No. 97061-422) in 1X PBS, + 3% goat serum (Sigma Aldrich – Cat No. G 9023-10ML). After blocking, devices were incubated at 4℃ overnight in VE-Cadherin and PECAM primary antibodies suspended in washing buffer: 0.5% BSA in 1X PBS. The next day, the primary antibody was pipetted out of the device and rinsed 5 times with washing buffer. Cells were

then incubated in Alexa Fluor 488 goat anti-rabbit (Thermo Fisher Scientific – Cat No. A-11008) and Alexa Fluor 555 goat anti-mouse (Thermo Fisher Scientific – Cat No. A-21422) secondary antibodies suspended in washing buffer at room temperature for 2 hours. Devices were rinsed and counter stained with DAPI and suspended in washing buffer for 1 hour at room temperature. Final washing consisted of washing with washing buffer three times and PBS twice. Devices were then imaged with our fluorescent microscope and processed using Matlab to acquire protein expression fluorescent intensities of the endothelial cell monolayers in the various conditions.

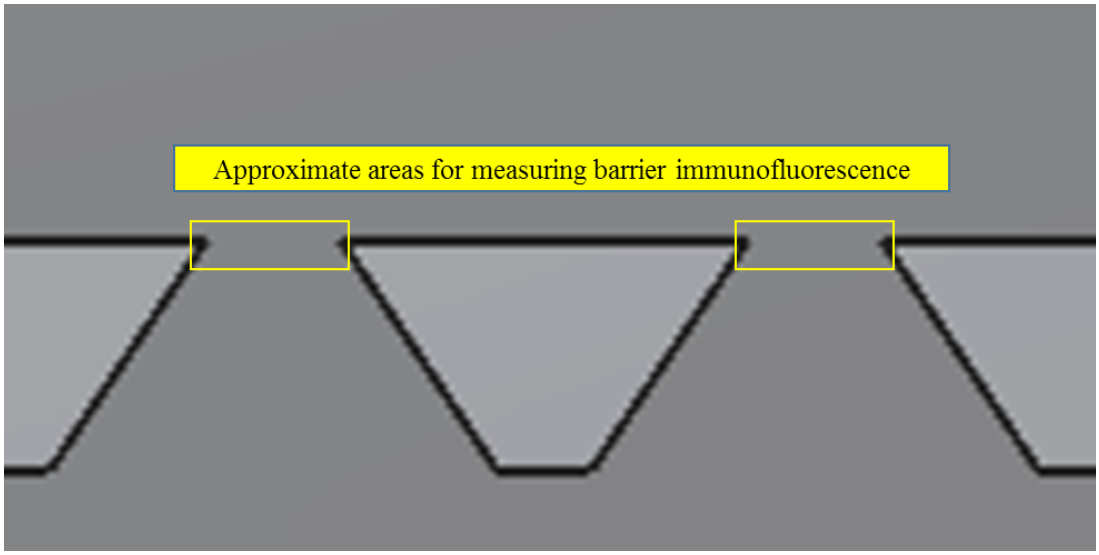

Figure 24 - Highlights the approximate areas where endothelial cells interact with the collagen protein matrix and form a monolayer for quantification.

A.5 Angiogenic Growth Measurement

Devices were given 24-48 hours to grow and form a monolayer against the collagen gel matrix. Cells were treated with 100ng/mL Hoechst for 45 minutes then imaged for a 0 hour timepoint. After imaging, devices were conditioned with: Vehicle, Aβ, VEGF or Aβ + VEGF with a VEGF gradient across the gel for the cells to grow towards. Conditions and

the VEGF gradient were suspended in VEGF-depleted EGM-2MV. Equal volumes were applied to both channels to ensure pressure equilibrium and prevent mechanical stimuli induced angiogenic sprouting. Figure 25 demonstrates the conditioning strategy for this experiment. Conditioned medium was replaced every 24 hours and cells were imaged again after 48 hours of conditioning. Angiogenic growth distances and branching were then quantified using Matlab.

A

Channel	Control	Aβ	VEGF	Aβ + VEGF
Cells Channel	Vehicle	300nM Aβ	20ng/mL VEGF	300nM Aβ 20ng/mL VEGF
Gradient Channel	20ng/mL VEGF	20ng/mL VEGF	40ng/mL VEGF	40ng/mL VEGF

B

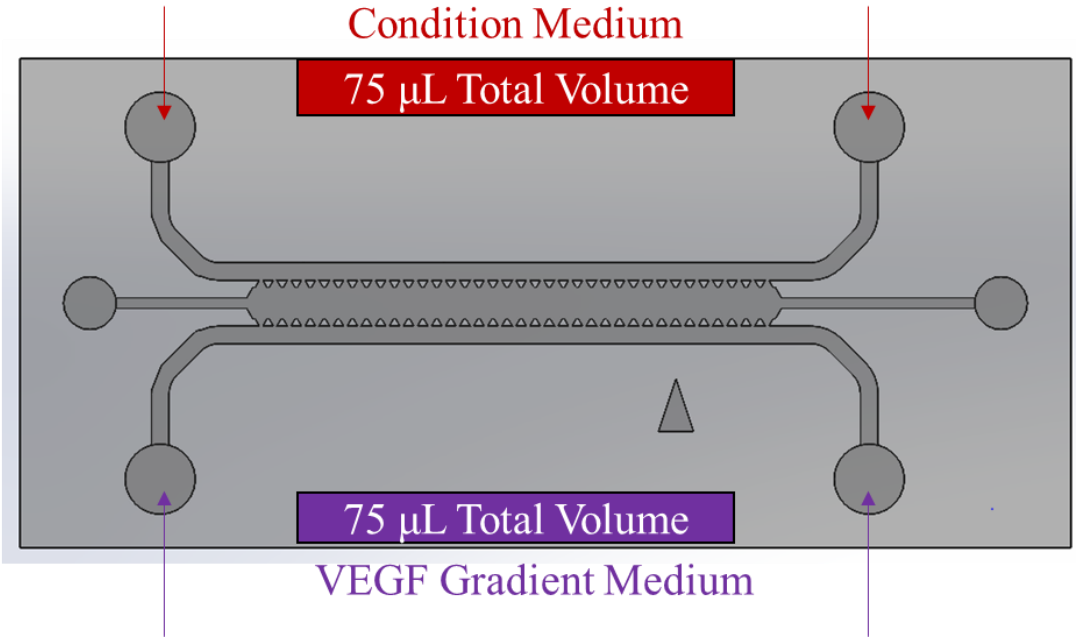

Figure 25 - (A) Table showing conditioning strategy for both channels in the angiogenesis assay. (B) Demonstration of pipetting strategy for maintaining pressure equilibrium during conditioning.

A.6 Phosphorylated Protein Analysis

Phospho-protein analysis was completed in both 2D and 3D cultures using similar protocols. 2D cultures were seeded at $1x10^5$ cells/mL in 6-well plates and grown to 90% confluence. Cells were starved with EBM-2 for 1 hour then were conditioned with: Vehicle, 300nM Aβ, 20ng/mL VEGF or 300nM Aβ + 20ng/mL VEGF for 15 minutes at 37℃. Plates were transported out of the incubator to an ice bucket and aspirated. Wells were rinsed with cold 1X PBS and aspirated again, followed by adding, to each well, 140 μL of Bio-plex lysis buffer: Cell Lysis Buffer (Bio-Rad – Cat No. 171304012), complete mini protease inhibitor tablet, Bio-Rad Factor 1 (Bio-Rad - in kit), Bio-Rad Factor 2 (Bio-Rad – in kit) and phenylmethylsulfonyl fluoride (Sigma Aldrich - Cat No. P7626-1G) in dimethyl sulfoxide (Sigma Aldrich – Cat No. D2650-100ML). Cells were detached with a cell scraper and lysates were transferred to micro-centrifuge tubes. Tubes were placed on an inverter at 4℃ for 10 minutes. Lysates were then centrifuged at 4℃ and carefully pipetted into different tubes to discard cell debris. Lastly, lysates were stored in a -80℃ freezer.

3D lysates were collected in a similar protocol. Cells were grown in both channels of devices and conditioned for 10 minutes. Devices were transferred to an ice bucket and rinsed for 2 minutes with cold 1X PBS. 40 μL of Bio-plex lysis buffer was added to each channel and incubated at 4℃ on ice for 1 hour. Lysates were then collected with the same protocol as 2D lysates.

To prepare lysates for analysis, a bicinchoninic acid assay (BCA, Thermo Fisher Scientific – Cat No. 23225) was conducted to identify protein concentration for each lysate.

Lysates were then used to conduct a linear range experiment for the 10-Plex MAPK/SAPK Signaling Magnetic Bead Kit (EMD Millipore – Cat No. 48-660MAG) with which 0.75µg and 1µg were found to be optimal loading masses for protein content in 2D and 3D lysates respectively. The MAPK/SAPK assay was completed by closely following the experimental protocol included with the kit and wells were read by our MAGPIX® (Luminex). All lysates were then used in the assay as above. All readings were processed in Matlab.

REFERENCES

[1] A. Alzheimer's, "2013 Alzheimer's disease facts and figures," *Alzheimers Dement,* vol. 9, no. 2, pp. 208-45, Mar 2013.

[2] K. L. Viola and W. L. Klein, "Amyloid beta oligomers in Alzheimer's disease pathogenesis, treatment, and diagnosis," *Acta Neuropathol,* vol. 129, no. 2, pp. 183-206, Feb 2015.

[3] P. Ballabh, A. Braun, and M. Nedergaard, "The blood-brain barrier: an overview: structure, regulation, and clinical implications," *Neurobiol Dis,* vol. 16, no. 1, pp. 1-13, Jun 2004.

[4] P. Grammas, "Neurovascular dysfunction, inflammation and endothelial activation: implications for the pathogenesis of Alzheimer's disease," *J Neuroinflammation,* vol. 8, p. 26, 2011.

[5] L. B. Wood *et al.,* "Identification of neurotoxic cytokines by profiling Alzheimer's disease tissues and neuron culture viability screening," *Scientific Reports,* vol. 5, Nov 2015, Art. no. 16622.

[6] C. Haass and D. J. Selkoe, "Soluble protein oligomers in neurodegeneration: lessons from the Alzheimer's amyloid beta-peptide," *Nature Reviews Molecular Cell Biology,* vol. 8, no. 2, pp. 101-112, Feb 2007.

[7] M. Goedert, "NEURODEGENERATION Alzheimer's and Parkinson's diseases: The prion concept in relation to assembled A beta, tau, and alpha-synuclein," *Science,* vol. 349, no. 6248, pp. 601-U135, Aug 7 2015.

[8] J. Godyn, J. Jonczyk, D. Panek, and B. Malawska, "Therapeutic strategies for Alzheimer's disease in clinical trials," *Pharmacological Reports,* vol. 68, no. 1, pp. 127-138, 2016.

[9] J. Sevigny *et al.,* "The antibody aducanumab reduces A beta plaques in Alzheimer's disease," *Nature,* vol. 537, no. 7618, pp. 50-56, Sep 2016.

[10] L. B. Wood, A. R. Winslow, and S. D. Strasser, "Systems biology of neurodegenerative diseases," *Integrative Biology,* vol. 7, no. 7, pp. 758-775, 2015.

[11] A. Carrano, J. J. M. Hoozemans, S. M. van der Vies, A. J. M. Rozemuller, J. van Horssen, and H. E. de Vries, "Amyloid Beta Induces Oxidative Stress-Mediated Blood-Brain Barrier Changes in Capillary Amyloid Angiopathy," *Antioxidants & Redox Signaling,* vol. 15, no. 5, pp. 1167-1178, Sep 2011.

[12] K. D. Rochfort, L. E. Collins, R. P. Murphy, and P. M. Cummins, "Downregulation of Blood-Brain Barrier Phenotype by Proinflammatory Cytokines Involves

NADPH Oxidase-Dependent ROS Generation: Consequences for Interendothelial Adherens and Tight Junctions," *Plos One,* vol. 9, no. 7, Jul 2014, Art. no. e101815.

[13] R. Sperling, "The potential of functional MRI as a biomarker in early Alzheimer's disease," *Neurobiology of Aging,* vol. 32, pp. S37-S43, Dec 2011.

[14] A. Carrano, J. J. M. Hoozemans, S. M. van der Vies, J. van Horssen, H. E. de Vries, and A. J. M. Rozemuller, "Neuroinflammation and Blood-Brain Barrier Changes in Capillary Amyloid Angiopathy," *Neurodegenerative Diseases,* vol. 10, no. 1-4, pp. 329-331, 2012.

[15] D. Zekry, C. Duyckaerts, J. Belmin, C. Geoffre, R. Moulias, and J. J. Hauw, "Cerebral amyloid angiopathy in the elderly: vessel walls changes and relationship with dementia," *Acta Neuropathologica,* vol. 106, no. 4, pp. 367-373, Oct 2003.

[16] H. A. D. Keage *et al.,* "Population studies of sporadic cerebral amyloid angiopathy and dementia: a systematic review," *Bmc Neurology,* vol. 9, Jan 2009, Art. no. 3.

[17] T. Malm, J. Koistinaho, and K. Kanninen, "Utilization of APPswe/PS1dE9 Transgenic Mice in Research of Alzheimer's Disease: Focus on Gene Therapy and Cell-Based Therapy Applications," *Int J Alzheimers Dis,* vol. 2011, p. 517160, 2011.

[18] J. Provias and B. Jeynes, "The role of the blood-brain barrier in the pathogenesis of senile plaques in Alzheimer's disease," *Int J Alzheimers Dis,* vol. 2014, p. 191863, 2014.

[19] J. D. Wang, E. S. Khafagy, K. Khanafer, S. Takayama, and M. E. ElSayed, "Organization of Endothelial Cells, Pericytes, and Astrocytes into a 3D Microfluidic in Vitro Model of the Blood-Brain Barrier," *Mol Pharm,* Jan 27 2016.

[20] C. Ruffer, A. Strey, A. Janning, K. S. Kim, and V. Gerke, "Cell-cell junctions of dermal microvascular endothelial cells contain tight and adherens junction proteins in spatial proximity," *Biochemistry,* vol. 43, no. 18, pp. 5360-9, May 11 2004.

[21] H. S. Lee *et al.,* "Hydrogen peroxide-induced alterations of tight junction proteins in bovine brain microvascular endothelial cells," *Microvascular Research,* vol. 68, no. 3, pp. 231-238, Nov 2004.

[22] R. C. McCarthy and D. J. Kosman, "Iron transport across the blood-brain barrier: development, neurovascular regulation and cerebral amyloid angiopathy," *Cellular and Molecular Life Sciences,* vol. 72, no. 4, pp. 709-727, Feb 2015.

[23] R. Minkeviciene *et al.,* "Age-related decrease in stimulated glutamate release and vesicular glutamate transporters in APP/PS1 transgenic and wild-type mice," *J Neurochem,* vol. 105, no. 3, pp. 584-94, May 2008.

[24] K. E. Biron, D. L. Dickstein, R. Gopaul, and W. A. Jefferies, "Amyloid triggers extensive cerebral angiogenesis causing blood brain barrier permeability and hypervascularity in Alzheimer's disease," *PLoS One,* vol. 6, no. 8, p. e23789, 2011.

[25] A. K. Stalder *et al.,* "Invasion of hematopoietic cells into the brain of amyloid precursor protein transgenic mice," *J Neurosci,* vol. 25, no. 48, pp. 11125-32, Nov 30 2005.

[26] P. Carmeliet and R. K. Jain, "Angiogenesis in cancer and other diseases," *Nature,* vol. 407, no. 6801, pp. 249-57, Sep 14 2000.

[27] P. Carmeliet, "Mechanisms of angiogenesis and arteriogenesis," *Nat Med,* vol. 6, no. 4, pp. 389-95, Apr 2000.

[28] B. S. Desai, J. A. Schneider, J. L. Li, P. M. Carvey, and B. Hendey, "Evidence of angiogenic vessels in Alzheimer's disease," *J Neural Transm (Vienna),* vol. 116, no. 5, pp. 587-97, May 2009.

[29] D. Paris, N. Patel, A. DelleDonne, A. Quadros, R. Smeed, and M. Mullan, "Impaired angiogenesis in a transgenic mouse model of cerebral amyloidosis," *Neurosci Lett,* vol. 366, no. 1, pp. 80-5, Aug 5 2004.

[30] R. Deane and B. V. Zlokovic, "Role of the blood-brain barrier in the pathogenesis of Alzheimer's disease," *Current Alzheimer Research,* vol. 4, no. 2, pp. 191-197, Apr 2007.

[31] D. Vestweber, "VE-cadherin: the major endothelial adhesion molecule controlling cellular junctions and blood vessel formation," *Arterioscler Thromb Vasc Biol,* vol. 28, no. 2, pp. 223-32, Feb 2008.

[32] D. Vestweber, M. Winderlich, G. Cagna, and A. F. Nottebaum, "Cell adhesion dynamics at endothelial junctions: VE-cadherin as a major player," *Trends Cell Biol,* vol. 19, no. 1, pp. 8-15, Jan 2009.

[33] A. Kalinowska and J. Losy, "PECAM-1, a key player in neuroinflammation," *Eur J Neurol,* vol. 13, no. 12, pp. 1284-90, Dec 2006.

[34] P. J. Newman and D. K. Newman, "Signal transduction pathways mediated by PECAM-1: new roles for an old molecule in platelet and vascular cell biology," *Arterioscler Thromb Vasc Biol,* vol. 23, no. 6, pp. 953-64, Jun 1 2003.

[35] K. Fujiwara, "Platelet endothelial cell adhesion molecule-1 and mechanotransduction in vascular endothelial cells," *J Intern Med,* vol. 259, no. 4, pp. 373-80, Apr 2006.

[36] H. M. DeLisser *et al.,* "Involvement of endothelial PECAM-1/CD31 in angiogenesis," *American Journal of Pathology,* vol. 151, no. 3, pp. 671-677, Sep 1997.

[37] G. Bazzoni and E. Dejana, "Endothelial cell-to-cell junctions: Molecular organization and role in vascular homeostasis," *Physiological Reviews,* vol. 84, no. 3, pp. 869-901, Jul 2004.

[38] R. E. Haddock *et al.*, "Endothelial coordination of cerebral vasomotion via myoendothelial gap junctions containing connexins 37 and 40," *American Journal of Physiology-Heart and Circulatory Physiology,* vol. 291, no. 5, pp. H2047-H2056, Nov 2006.

[39] P. Carmeliet and D. Collen, "Molecular basis of angiogenesis. Role of VEGF and VE-cadherin," *Ann N Y Acad Sci,* vol. 902, pp. 249-62; discussion 262-4, May 2000.

[40] B. E. Sumpio *et al.*, "MAPKs (ERK1/2, p38) and AKT can be phosphorylated by shear stress independently of platelet endothelial cell adhesion molecule-1 (CD31) in vascular endothelial cells," *Journal of Biological Chemistry,* vol. 280, no. 12, pp. 11185-11191, Mar 2005.

[41] J. J. Zhang, R. J. Kelm, P. Biswas, M. Kashgarian, and J. A. Madri, "PECAM-1 modulates thrombin-induced tissue factor expression on endothelial cells," *Journal of Cellular Physiology,* vol. 210, no. 2, pp. 527-537, Feb 2007.

[42] S. Marco and S. D. Skaper, "Amyloid beta-peptide(1-42) alters tight junction protein distribution and expression in brain microvessel endothelial cells," *Neuroscience Letters,* vol. 401, no. 3, pp. 219-224, Jul 2006.

[43] M. Labelle *et al.*, "Vascular endothelial cadherin promotes breast cancer progression via transforming growth factor beta signaling," *Cancer Res,* vol. 68, no. 5, pp. 1388-97, Mar 1 2008.

[44] P. Grammas and R. Ovase, "Inflammatory factors are elevated in brain microvessels in Alzheimer's disease," *Neurobiol Aging,* vol. 22, no. 6, pp. 837-42, Nov-Dec 2001.

[45] R. von Bernhardi, L. Eugenn-von Bernhardi, and J. Eugenin, "Microglial cell dysregulation in brain aging and neurodegeneration," *Frontiers in Aging Neuroscience,* vol. 7, Jul 2015, Art. no. 124.

[46] L. B. Wood, R. Ge, R. D. Kamm, and H. H. Asada, "Nascent vessel elongation rate is inversely related to diameter in in vitro angiogenesis," *Integr Biol (Camb),* vol. 4, no. 9, pp. 1081-9, Sep 2012.

[47] N. J. Abbott, L. Ronnback, and E. Hansson, "Astrocyte-endothelial interactions at the blood-brain barrier," *Nat Rev Neurosci,* vol. 7, no. 1, pp. 41-53, Jan 2006.

[48] M. A. Farhan, K. Carmine-Simmen, J. D. Lewis, R. B. Moore, and A. G. Murray, "Endothelial Cell mTOR Complex-2 Regulates Sprouting Angiogenesis," *PLoS One,* vol. 10, no. 8, p. e0135245, 2015.

[49] M. Shibuya, "Vascular Endothelial Growth Factor (VEGF) and Its Receptor (VEGFR) Signaling in Angiogenesis: A Crucial Target for Anti- and Pro-Angiogenic Therapies," *Genes Cancer,* vol. 2, no. 12, pp. 1097-105, Dec 2011.

[50] D. A. Do TM, Alata W, Calon F, Nicolic S, Schermann JM, Farinotti R, Bourasset F, "Age-Dependent Regulation of the Blood-Brain Barrier Influx/Efflux Equilibrium of Amyloid-β Peptide in a Mouse Model of Alzheimer's Disease (3xTg-AD)," *Journal of Alzheimer's Disease,* vol. 49, no. 2, p. 13, 2015.

[51] T. M. Do *et al.*, "Altered cerebral vascular volumes and solute transport at the blood–brain barriers of two transgenic mouse models of Alzheimer's disease," *Neuropharmacology,* vol. 81, pp. 311-317, 6// 2014.

[52] E. Urich, C. Patsch, S. Aigner, M. Graf, R. Iacone, and P. O. Freskgard, "Multicellular Self-Assembled Spheroidal Model of the Blood Brain Barrier," *Scientific Reports,* vol. 3, Mar 2013, Art. no. 1500.

[53] E. Urich, C. Patsch, S. Aigner, M. Graf, R. Iacone, and P. O. Freskgard, "Multicellular self-assembled spheroidal model of the blood brain barrier," *Sci Rep,* vol. 3, p. 1500, 2013.

[54] R. Booth and H. Kim, "Characterization of a microfluidic in vitro model of the blood-brain barrier (muBBB)," *Lab Chip,* vol. 12, no. 10, pp. 1784-92, Apr 24 2012.

[55] A. L. Placone, P. M. McGuiggan, D. E. Bergles, H. Guerrero-Cazares, A. Quinones-Hinojosa, and P. C. Searson, "Human astrocytes develop physiological morphology and remain quiescent in a novel 3D matrix," *Biomaterials,* vol. 42, pp. 134-43, Feb 2015.

[56] A. Wolff, M. Antfolk, B. Brodin, and M. Tenje, "In Vitro Blood-Brain Barrier Models-An Overview of Established Models and New Microfluidic Approaches," *J Pharm Sci,* vol. 104, no. 9, pp. 2727-46, Sep 2015.

[57] A. P. Adam, A. L. Sharenko, K. Pumiglia, and P. A. Vincent, "Src-induced tyrosine phosphorylation of VE-cadherin is not sufficient to decrease barrier function of endothelial monolayers," *J Biol Chem,* vol. 285, no. 10, pp. 7045-55, Mar 5 2010.

[58] E. Kniazeva and A. J. Putnam, "Endothelial cell traction and ECM density influence both capillary morphogenesis and maintenance in 3-D," *American Journal of Physiology-Cell Physiology,* vol. 297, no. 1, pp. C179-C187, Jul 2009.

[59] Y. Zheng *et al.*, "In vitro microvessels for the study of angiogenesis and thrombosis," *Proc Natl Acad Sci U S A,* vol. 109, no. 24, pp. 9342-7, Jun 12 2012.

[60] S. J. Kim, R. Yokokawa, and S. Takayama, "Analyzing threshold pressure limitations in microfluidic transistors for self-regulated microfluidic circuits," *Appl Phys Lett,* vol. 101, no. 23, p. 234107, Dec 3 2012.

[61] M. De Bock *et al.*, "Endothelial calcium dynamics, connexin channels and blood-brain barrier function," *Progress in Neurobiology*, vol. 108, pp. 1-20, Sep 2013.

[62] H. Y. Wu *et al.*, "Amyloid beta induces the morphological neurodegenerative triad of spine loss, dendritic simplification, and neuritic dystrophies through calcineurin activation," *J Neurosci*, vol. 30, no. 7, pp. 2636-49, Feb 17 2010.

[63] H. LeVine, "Alzheimer's beta-peptide oligomer formation at physiologic concentrations," *Analytical Biochemistry*, vol. 335, no. 1, pp. 81-90, Dec 2004.

[64] M. Anguiano *et al.*, "Characterization of three-dimensional cancer cell migration in mixed collagen-Matrigel scaffolds using microfluidics and image analysis," *Plos One*, vol. 12, no. 2, Feb 2017, Art. no. e0171417.

[65] W. C. Chen, H. H. Lin, and M. J. Tang, "Regulation of proximal tubular cell differentiation and proliferation in primary culture by matrix stiffness and ECM components," *American Journal of Physiology-Renal Physiology*, vol. 307, no. 6, pp. F695-F707, Sep 2014.

[66] S. L. Duffy and J. T. Murphy, "Colorimetric assay to quantify macromolecule diffusion across endothelial monolayers," *Biotechniques*, vol. 31, no. 3, pp. 495-6, 498, 500-1, Sep 2001.

[67] R. T. Bartus *et al.*, "Controlled modulation of BBB permeability using the bradykinin agonist, RMP-7," *Experimental Neurology*, vol. 142, no. 1, pp. 14-28, Nov 1996.

[68] A. Beaumont *et al.*, "The permissive nature of blood brain barrier (BBB) opening in edema formation following traumatic brain injury," in *Brain Edema Xi*, vol. 76, A. D. Mendelow *et al.*, Eds. (Acta Neurochirurgica Supplementa, 2000, pp. 125-129.

[69] P. M. Abdul-Muneer, N. Chandra, and J. Haorah, "Interactions of Oxidative Stress and Neurovascular Inflammation in the Pathogenesis of Traumatic Brain Injury," *Molecular Neurobiology*, vol. 51, no. 3, pp. 966-979, Jun 2015.

[70] N. S. Patel *et al.*, "Alzheimer's beta-amyloid peptide blocks vascular endothelial growth factor mediated signaling via direct interaction with VEGFR-2," *J Neurochem*, vol. 112, no. 1, pp. 66-76, Jan 2010.

[71] S. P. Yang, B. O. Kwon, Y. S. Gho, and C. B. Chae, "Specific interaction of VEGF165 with beta-amyloid, and its protective effect on beta-amyloid-induced neurotoxicity," *J Neurochem*, vol. 93, no. 1, pp. 118-27, Apr 2005.

[72] S. Koch, S. Tugues, X. Li, L. Gualandi, and L. Claesson-Welsh, "Signal transduction by vascular endothelial growth factor receptors," *Biochem J*, vol. 437, no. 2, pp. 169-83, Jul 15 2011.

[73] E. Vandenbroucke, D. Mehta, R. Minshall, and A. B. Malik, "Regulation of endothelial junctional permeability," *Control and Regulation of Transport Phenomena in the Cardiac System,* vol. 1123, pp. 134-145, 2008.

[74] D. Paris *et al.*, "Inhibition of angiogenesis by Abeta peptides," *Angiogenesis,* vol. 7, no. 1, pp. 75-85, 2004.

[75] J. Evans *et al.*, "Arachidonic acid induces brain endothelial cell apoptosis via p38-MAPK and intracellular calcium signaling," *Microvascular Research,* vol. 98, pp. 145-158, Mar 2015.

[76] A. Y. Sun, M. Liu, X. V. Nguyen, and G. Y. Bing, "p38 MAP kinase is activated at early stages in Alzheimer's disease brain," *Experimental Neurology,* vol. 183, no. 2, pp. 394-405, Oct 2003.

[77] D. Raman, P. J. Baugher, Y. M. Thu, and A. Richmond, "Role of chemokines in tumor growth," *Cancer Lett,* vol. 256, no. 2, pp. 137-65, Oct 28 2007.

[78] K. M. Jorgensen *et al.*, "Untangling the intracellular signalling network in cancer - A strategy for data integration in acute myeloid leukaemia," *Journal of Proteomics,* vol. 74, no. 3, pp. 269-281, Mar 2011.

[79] P. Kopesky *et al.*, "Autocrine signaling is a key regulatory element during osteoclastogenesis," *Biology Open,* vol. 3, no. 8, pp. 767-776, Aug 2014.

[80] D. J. Glass, "Skeletal muscle hypertrophy and atrophy signaling pathways," *Int J Biochem Cell Biol,* vol. 37, no. 10, pp. 1974-84, Oct 2005.

[81] A. Salemme *et al.*, "Anti-inflammatory effects and antioxidant activity of dihydroasparagusic acid in lipopolysaccharide-activated microglial cells," *Brain Research Bulletin,* vol. 120, pp. 151-158, Jan 2016.

[82] M. Elahy *et al.*, "Blood-brain barrier dysfunction developed during normal aging is associated with inflammation and loss of tight junctions but not with leukocyte recruitment," *Immunity & Ageing,* vol. 12, Mar 7 2015, Art. no. 2.

[83] D. M. Mosser and X. Zhang, "Activation of murine macrophages," *Curr Protoc Immunol,* vol. Chapter 14, p. Unit 14 2, Nov 2008.

[84] A. Mantovani, A. Sica, S. Sozzani, P. Allavena, A. Vecchi, and M. Locati, "The chemokine system in diverse forms of macrophage activation and polarization," *Trends Immunol,* vol. 25, no. 12, pp. 677-86, Dec 2004.

[85] S. Okizaki *et al.*, "Vascular Endothelial Growth Factor Receptor Type 1 Signaling Prevents Delayed Wound Healing in Diabetes by Attenuating the Production of IL-1beta by Recruited Macrophages," *Am J Pathol,* vol. 186, no. 6, pp. 1481-98, Jun 2016.

[86] J. Li *et al.*, "PR39, a peptide regulator of angiogenesis," *Nat Med*, vol. 6, no. 1, pp. 49-55, Jan 2000.

[87] G. M. Whitesides, E. Ostuni, S. Takayama, X. Y. Jiang, and D. E. Ingber, "Soft lithography in biology and biochemistry," *Annual Review of Biomedical Engineering*, vol. 3, pp. 335-373, 2001.